SELF-SIMILAR BLOW-UP IN HIGHER-ORDER SEMILINEAR PARABOLIC EQUATIONS *

C. J. BUDD †, V.A. GALAKTIONOV ‡, AND J. F. WILLIAMS §

Abstract. We study the Cauchy problem in $\mathbf{R} \times \mathbf{R}_+$ for one-dimensional $2m$th-order ($m > 1$) semilinear parabolic PDEs of the form ($D_x = \partial/\partial x$)

$$u_t = (-1)^{m+1} D_x^{2m} u + |u|^{p-1} u, \text{ where } p > 1, \quad \text{and} \quad u_t = (-1)^{m+1} D_x^{2m} u + e^u$$

with bounded initial data $u_0(x)$. Specifically, we are interested in the those solutions which blow up at the origin in a finite time T. We show that in contrast to the solutions of the classical second-order parabolic equations $u_t = u_{xx} + u^p$ and $u_t = u_{xx} + e^u$ from Combustion Theory, the blow-up in their higher-order counterparts is asymptotically *self-similar*. In particular, there exist exact non-trivial self-similar blow-up solutions $u_*(x,t) = (T-t)^{-1/(p-1)} f(y)$, in the case of the polynomial non-linearity and $u(x,t) = -\ln(T-t) + f(y)$ for the exponential non-linearity, where $y = x/(T-t)^{1/2m}$ is the backward higher-order heat kernel variable. The profiles $f(y)$ satisfy related semilinear ODEs which share the same non self-adjoint higher-order linear differential operators. We show that there are *at least* $2\lfloor m/2 \rfloor$ non-trivial self-similar solutions to the full PDEs. Numerical solution of the ODEs for $m = 2$ and 3 supports this and the time dependent solutions of the PDEs for $m = 2$ are then studied by using a scale invariant adaptive numerical method. It is shown that those functions $f(y)$ which have the simplest spatial shape (e.g., a single maximum) correspond to *stable* self-similar solutions. A further countable subset of non-similarity blow-up patterns can be constructed by linearization and matching with similarity solutions of a first-order Hamilton-Jacobi equation.

Key words. Semilinear parabolic equation, blow-up, asymptotic behaviour, similarity solutions

AMS subject classifications. 35K55, 35K65

1. Introduction.

Scaling and self-similarity have been known since the 1930's to give a fundamental insight into many systems which develop singularities in finite time. A general treatment of blow-up processes naturally occurred in the 1930's - 1950's in the context of N.N. Semenov's chain reaction theory, adiabatic explosion and combustion theory (the first blow-up result by O.M. Todes (1933)), see [25] and [46]. On the other hand, in the same period there was a strong influence from the study of blow-up singularities in gas dynamics, in particular, the intense explosion (focusing) problem, admitting similarity solutions of the second kind, was considered by K. Bechert, K.G. Guderley and L.I. Sedov in the 1940's; see [4], p. 127, and [47]. Another classical area of blow-up processes in the 1960's is nonlinear optics, where the main model is the nonlinear (cubic) Schrödinger equation defined in $\mathbf{R}^2$ or $\mathbf{R}^3$ which admits blowing up self-focusing solutions; see references in the book [41].

1.1. On second-order semilinear and quasilinear heat equations from Combustion Theory: singularity formation.

Because of their importance to many applications, canonical equations from Combustion Theory such as the non-stationary semilinear one-dimensional *Frank-Kamenetskii equation* [19] (the solid fuel

---

[*] Research supported by the TMR network ERB FMRX CT98-0201 and RTN network HPRN-CT-2002-00274

[†] Department of Mathematical Sciences, University of Bath, Bath BA2 7AY, UK (`cjb@maths.bath.ac.uk`).

[‡] Department of Mathematical Sciences, University of Bath, Bath BA2 7AY, UK and Keldysh Institute of Applied Mathematics, Miusskaya Sq. 4, 125047 Moscow, RUSSIA, (`vag@maths.bath.ac.uk`).

[§] Centrum voor Wiskunde en Informatica, Postbus 94079, 1090 GB, Amsterdam, NL (`williams@cwi.nl`).

model [46])

$$u_t = u_{xx} + e^u, \quad x \in \mathbf{R}, \;\; t > 0, \tag{1.1}$$

and its counterpart with a power nonlinearity

$$u_t = u_{xx} + u^p, \quad x \in \mathbf{R}, \;\; t > 0 \quad \text{with exponent } p > 1 \quad (u(x,t) \geq 0) \tag{1.2}$$

have been well studied for the past thirty years. It is known that these both exhibit singularities in finite time. While exact self-similar solutions are known to exist for the related second-order reaction-diffusion *quasilinear* problems (see references to Chapter 4 in [39] and [8])

$$u_t = (|u_x|^\sigma u_x)_x + e^u \quad \text{or} \quad u_t = (u^\sigma u_x)_x + u^p \quad \text{with} \;\; \sigma > 0, \tag{1.3}$$

it is somewhat paradoxical that none exist for the above semilinear problems. Instead, the generic stable asymptotic blow-up behaviour is described by approximate similarity solutions satisfying first-order Hamilton-Jacobi equations, see the references in the books [5, 39] and the surveys [34, 23]. For example, in the quasilinear problem (1.3) with the power non-linearity u^p, for any $p > 1$ and $\sigma > 0$, there exists an *exact* non-trivial self-similar solution of the form

$$u_S(x,t) = (T-t)^{-1/(p-1)} f(y), \quad y = x/(T-t)^{(p-1-\sigma)/2(p-1)}, \tag{1.4}$$

where T is the finite blow-up time, f is not identically constant and solves a related ODE; see Chapter 4 in [39].

In comparison, for the semilinear equation (1.2), looking for the same similarity solution

$$u_S(x,t) = (T-t)^{-1/(p-1)} f(y), \quad y = x/(T-t)^{1/2}$$

yields that for the corresponding ODE the only non-zero similarity profile is the trivial constant one $f \equiv \beta^\beta$, where $\beta = 1/(p-1)$. Such nonexistence result are known from the 1970's, see [30] ($p = 3$), [1] ($p > 1$) and [26] for the corresponding equation in $\mathbf{R}^N$ with $1 < p \leq (N+2)/(N-2)_+$. This means that for a wide "dense" subset of general solutions $u(x,t)$ blowing up at $t = T$ at the origin $x = 0$, the similarity rescaling satisfies [22, 27]

$$\theta(y,t) \equiv (T-t)^{1/(p-1)} u(x,t) \to \beta^\beta \quad \text{as } t \to T^-$$

uniformly on compact subset in y. The spatial variation of the blow-up solutions can be observed on larger subsets, and the generic asymptotic behaviour is as follows:

$$u(x,t) = [(p-1)(T-t)(1 + C_* \eta^2)]^{-1/(p-1)}(1 + o(1)) \tag{1.5}$$

uniformly on compact subsets in $\eta = x/[(T-t)|\ln(T-t)|]^{1/2}$, where the constant $C_* = (p-1)/4p$ does not depend on initial data (nor, in fact, on the space dimension). The non scaling-invariant "hot-spot variable" η with an extra logarithmic factor was first formally derived in 1972 [30] and was rigorously established twenty years later, see [7, 18, 29, 36, 43, 44] and the survey [23]. The stable behaviour (1.5) is essentially equivalent to the fact that the ODE for the self-similar solutions, which is obtained by a symmetry reduction of the original PDE, has no solution (other than the constant one) with an appropriate decay rate at infinity. Comparing (1.4) and (1.5) shows that nonexistence of non-trivial ODE similarity profiles implies a fundamental change of the basic spatial scale of singularity formation phenomena. The observation that the blow-up behaviour of these second order problems is only approximately self-similar with a new logarithmically perturbed backward heat kernel variable is an essential feature of many related reaction diffusion problems and the corresponding parabolic equations under consideration.

1.2. Main higher-order semilinear models, results and plan of the paper. Higher-order semilinear parabolic equations arise in many physical applications such as thin film theory, convection-explosion theory, lubrication theory, flame and wave propagation (the Kuramoto-Sivashinsky equation and the extended Fisher-Kolmogorov equation), phase transition at critical Lifschitz points, bi-stable systems and applications to structural mechanics. The effect of fourth order terms on self-focusing problems in nonlinear optics has also recently been considered in [17, 6]. Indeed, fourth (and higher) order terms are increasingly recognized as being significant in many physical models, this has lead to the burgeoning literature including the recent book [38] which lists a number of models and references. Therefore, it is important to know if higher-order semilinear equations exhibit analogous singularity behaviour to their classical second-order counterparts where the exact self-similar behaviour is unavailable.

In the present paper we show that the higher-order generalizations of the second order model (1.1), the *extended Frank-Kamenetskii equation*,

$$u_t = (-1)^{m+1} D_x^{2m} u + e^u, \quad x \in \mathbf{R},\ t > 0 \quad (D_x = \partial/\partial x), \tag{1.6}$$

and of (1.2),

$$u_t = (-1)^{m+1} D_x^{2m} u + |u|^{p-1} u, \quad x \in \mathbf{R},\ t > 0, \tag{1.7}$$

have self-similar blow-up solutions and hence their evolution is somewhat simpler than in the case $m = 1$, though, of course, for $m > 1$ the problem of rigorous justification of the results becomes much more delicate. Fundamentally, we would like to understand the importance of the semilinear structure in these equations (1.6) and (1.7) and its role in self-similarity. This study is an attempt to further mathematical understanding of higher-order parabolic equations and, in particular, the corresponding singularity formation phenomena, an area of increasing physical and mathematical importance. In particular, a model, admitting blow-up, from convection-explosion theory has been described in [32] and takes the form

$$u_t = -u_{xxxx} - [(2 - (u_x)^2) u_x]_x - \alpha u + q e^{su}. \tag{1.8}$$

Here the formation of such finite time singularities was shown to be self-similar [24] with a number of analogous properties to the generic equations (1.7) and (1.6).

In Section 2 we introduce the relevant mathematical definitions, formulation of similarity variables and rescaled equations. In Section 3 we present the properties of the underlying linearized operator which governs the "dynamics" of both equations (1.6) and (1.7) near certain blow-up solutions.

In Section 4 we consider an extension of the linearized problem which makes clear the structure of the subset of nonlinear evolution patterns. In particular, we analyze bifurcation points associated to the linearized operator and present an argument for the existence of self-similar solutions. This analytic argument is strengthened with numerical and asymptotic evidence. Section 5 is devoted to the asymptotic behaviour of the solutions close to bifurcation points.

Lastly, in Sections 6 and 7 we construct the blow-up profiles asymptotically and compare them with numerical solutions of both the ODE for the self-similar profile and rescaled profiles from simulations of the full PDEs.

This paper is mainly devoted to the study of self-similar blow-up for higher-order semilinear parabolic equations, though we discuss some related centre manifold structures. Countable spectra of other blow-up patterns which are approximately self-similar and are constructed by matching of different asymptotic regions are studied in [20], see also [24] for equation (1.8).

2. Finite time blow-up solutions and similarity variables.

2.1. Blow-up solutions. Central to singularity formation phenomena for $2m$th-order reaction-diffusion equations is the concept of finite time blow-up, where the solution of the Cauchy problem with uniformly bounded initial data $u_0(x)$ becomes unbounded at some time $T \in \mathbf{R}_+$ in the sense that $u(x,t)$ exists and is classical on any time-interval $[0,T']$ with $T' \in (0,T)$ and

$$\sup_{x \in \mathbf{R}} |u(x,t)| \to \infty \quad \text{as } t \to T^-. \tag{2.1}$$

Finite time blow-up for higher-order semilinear and quasilinear parabolic equations is well known from the 1970's. There are several techniques for proving blow-up including the concavity methods [34], test functions methods [37], see also [14] and references therein, and an extension of Kaplan's idea based on derivation of an ordinary differential inequality for the first Fourier coefficient of the solutions [21, 10].

2.2. Similarity variables and rescaled PDEs. Finite time blow-up singularities involve a delicate balance between the spatial and temporal derivatives and the reaction terms driving the blow-up. This balance is made naturally apparent by considering the scaling invariance of the underlying PDE. This scaling structure is also important for the numerical methods employed in integrating the full PDE, see Section 5.

Because of their semilinear structure, the PDEs (1.6) and (1.7) have similar scaling symmetries, so that (1.7) is invariant with respect to the scaling transformations

$$t \mapsto \lambda t, \quad x \mapsto \lambda^{1/2m} x, \quad u \mapsto \lambda^{-1/(p-1)} u \quad \text{for all } \lambda > 0,$$

while (1.6) is invariant under the group of transformations

$$t \mapsto \lambda t, \quad x \mapsto \lambda^{1/2m} x, \quad u \mapsto u - \ln \lambda.$$

Without loss of generality, we may assume that the solution $u(x,t)$ blows up at finite time $t = T$ in the sense of (2.1) and the blow-up set $B[u_0]$ defined by

$$B[u_0] = \{x \in I : \text{ there exist } \{x_k\} \to x, \ \{t_k\} \to T^- \text{ such that } u(x_k,t_k) \to \infty\} \tag{2.2}$$

contains the origin, $0 \in B[u_0]$. Motivated by this assumption and looking for invariants of the above groups of transformations, we introduce the following self-similar spatial variable:

$$y = x/(T-t)^{1/2m} : \mathbf{R} \to \mathbf{R}, \quad t \in [0,T),$$

and the new time variable

$$\tau = -\ln(T-t) : (0,T) \to (\tau_0, \infty) \quad \text{with } \tau_0 = -\ln T.$$

Then for the polynomial nonlinearity we define a new dependent variable (the rescaled solution) $\theta(y,\tau)$ by

$$u(x,t) = (T-t)^{-1/(p-1)}\theta(y,\tau) \tag{2.3}$$

and for the exponential nonlinearity by

$$u(x,t) = -\ln(T-t) + \theta(y,\tau). \tag{2.4}$$

Rescaling (1.7) in terms of the new variables by substituting (2.3), we obtain the following PDE for the rescaled solution θ:

$$\theta_\tau = \boldsymbol{\mathcal{L}}\theta + G_p(\theta), \quad y \in \mathbf{R},\ \tau > \tau_0, \quad \text{where } G_p(\theta) = |\theta|^{p-1}\theta - \theta/(p-1), \tag{2.5}$$

and the linear differential operator $\boldsymbol{\mathcal{L}}$ is given by

$$\boldsymbol{\mathcal{L}} \equiv (-1)^{m+1}D_y^{2m} - \frac{1}{2m}D_y. \tag{2.6}$$

Similarly, rescaling (1.6) leads to the PDE

$$\theta_\tau = \boldsymbol{\mathcal{L}}\theta + G_e(\theta), \quad y \in \mathbf{R},\ \tau > \tau_0, \quad \text{where } G_e(\theta) = e^\theta - 1. \tag{2.7}$$

It is important that unlike the well understood case $m = 1$, for any $m > 1$ the operators on the right-hand sides *are not potential* and equations (2.5) and (2.7) do not possess Lyapunov functions.

2.3. Preliminaries: local and asymptotic properties of self-similar solutions. Exact (not just asymptotic) self-similar solutions are those which are invariant under the group of transformations, i.e., correspond to suitable stationary solutions $\theta(y)$ which are independent of the rescaled time τ. Any exact self-similar solution to (1.7) takes the form

$$u_S(x,t) = (T-t)^{-1/(p-1)}f(y), \tag{2.8}$$

where $f(y)$ satisfies the ODE

$$\boldsymbol{\mathcal{L}}f + G_p(f) = 0 \quad \text{in } \mathbf{R}. \tag{2.9}$$

It is natural to impose the symmetry conditions at the origin

$$f'(0) = f'''(0) = ... = f^{(2m-1)}(0) = 0. \tag{2.10}$$

Then a stable (generic) self-similar solution with a suitable similarity profile f in (2.8) means that for a sufficiently wide and dense subset of global symmetric non-stationary solutions to (2.5), there holds

$$\theta(y,\tau) \to f(y) \quad \text{as} \quad \tau \to \infty$$

in a suitable metric. For such a stable similarity solution (2.8) to have non-vanishing trace in the limit $t \to T^-$ and to rule out constant solutions, we need to impose a special decay condition on $f(y)$ as $y \to \infty$. In particular, we will demand that there exists a finite limit $u(x,t) \to u(x,T^-)$ as $t \to T^-$ for arbitrarily small fixed $|x| > 0$.

2.3.1. Asymptotic behaviour at infinity. First, we need to describe possible asymptotics of small solutions to (2.5) satisfying $f(y) \to 0$ as $y \to +\infty$. Consider the linearization of (2.9) about $f = 0$,

$$\mathcal{L}f - f/(p-1) = 0, \quad y > 0. \tag{2.11}$$

Setting $z = y^\nu$ with $\nu = 2m/(2m-1)$ reduces it to

$$f^{(2m)} - a_1 f' - a_2 z^{-1} f + \mathbf{B}(z) f = 0, \tag{2.12}$$

where $a_1 = (-1)^{m+1}\nu^{1-2m}/2m$, $a_2 = (-1)^{m+1}\nu^{-2m}/(p-1)$ and

$$\mathbf{B}(z)f = \sum_{j=1}^{2m-1} \gamma_j z^{j-2m} f^{(j)}$$

is a linear operator with bounded coefficients as $z \to \infty$, where the first coefficient of derivative f' is of order $O(z^{1-2m})$. By the perturbation theory of higher-order linear ODEs (see Chapters III - V in [12]), we have that the leading terms of exponentially decaying solutions are described by the operator in (2.12) with constant coefficients,

$$f^{(2m)} - a_1 f' = 0. \tag{2.13}$$

Setting $f = e^{pz}$, $p \neq 0$, gives the characteristic equation $p^{2m} - a_1 p = 0$, whence

$$p^{2m-1} = a_1 = (-1)^{m+1}/2m\nu^{2m-1} \equiv \rho_0^{2m-1}(-1)^{m+1}, \quad \text{where } \rho_0 > 0. \tag{2.14}$$

For any $m \geq 1$, there exist $2m-1$ roots $\{p_0, p_1, ..., p_{2m-2}\}$ given by

$$p_k = \rho_0 e^{i(2k+1)\pi/(2m-1)}, \;\; m = 2l; \quad p_k = \rho_0 e^{i2\pi k/(2m-1)}, \;\; m = 2l+1, \tag{2.15}$$

where $m-1$ roots have negative real parts ($\mathrm{Re}\, p_k < 0$). These correspond to $l \leq k \leq 3l-2$ for even $m = 2l$ and $l+1 \leq k \leq 3l$ for odd $m = 2l+1$. The linearized equation (2.11) has a κ_m-dimensional subspace of exponentially decaying solutions as $y \to \infty$, where $\kappa_m = 2m-3$ for m even and $\kappa_m = 2(m-1)$ for m odd. For the second-order case $m = 1$, it is empty.

On the other hand, equation (2.12) admits a solution with algebraic decay (rather than exponential) as $z \to \infty$ described by the first-order operator

$$-a_1 f' - a_2 z^{-1} f = 0 \quad \Longrightarrow \quad f(z) = c\, z^{-(2m-1)/(p-1)}.$$

Existence of solutions with such a decay for the perturbed equation (2.12) is established by a standard expansion analysis by calculating solutions via Kummer-type series converging uniformly for $z \gg 1$. For the linearized equation (2.11), the leading order behaviour is algebraic,

$$f(y) = C|y|^{2m/(p-1)}(1 + o(1)) \quad \text{as } y \to \infty, \text{ with } C \neq 0. \tag{2.16}$$

In summary, these results yield that equation (2.11) admits an

$$\kappa_m + 1\text{-dimensional subset of admissible solutions as } y \to \infty. \tag{2.17}$$

Actually, for the nonlinear equation (2.9) we are going to look for profiles $f(y)$ having the algebraic decay (2.16). Then for such similarity solutions (2.8), the limit-time profile is bounded for any $x \neq 0$ and is given by

$$u_S(x, T^-) = C|x|^{-2m/(p-1)}.$$

Asymptotic and numerical computations suggest that the solutions of (2.9) which satisfy (2.16) are *isolated* and that the constant C plays a role of a *nonlinear* eigenvalue. In Section 5 we give an asymptotic formula for one value of C valid in a certain limit.

Likewise for (1.6), the self-similar solution is given by

$$u_S(x,t) = -\ln(T-t) + f(y), \tag{2.18}$$

where the function $f(y)$ satisfies the ODE

$$\mathcal{L}f + G_e(f) = 0 \tag{2.19}$$

with the symmetry conditions (2.10). We look for similarity profiles $f(y) \to -\infty$ "slowly" as $y \to \infty$. The limit $\lim_{f\to-\infty} G_e(f) = -1$, so we first consider the "linearized" equation

$$\mathcal{L}f = 1. \tag{2.20}$$

Setting $f(y) = -2m\ln y + g(y)$ for $y > 0$, we obtain

$$\mathcal{L}g = 1 + 2m\,\mathcal{L}\ln y \;=\; 2m(-1)^{m+1}D_y^{2m}\ln y = O(y^{-2m}) \quad \text{as } y \to +\infty. \tag{2.21}$$

As above, the homogeneous equation $\mathcal{L}g = 0$ has a κ_m-dimensional subspace of exponentially decaying solutions. The non-homogeneous equation (2.21) has solutions $g(y) = C + o(1)$ as $y \to +\infty$, so that (2.17) holds for equation (2.20) admitting a $\kappa_m + 1$-dimensional subset of solutions satisfying

$$f(y) = -2m\ln|y| + C + o(1) \quad \text{as} \quad y \to \infty. \tag{2.22}$$

In this case the limit-time profile is given by

$$u_S(x,T^-) = -2m\ln|x| + C,$$

where again the constant $C \in \mathbf{R}$ is a certain isolated nonlinear eigenvalue which can be approximated asymptotically.

Obviously, ODEs (2.9) and (2.19) admit constant solutions $f^*_{p,e}$ satisfying

$$G_p(f_p^*) = 0,\ f_p^* = \beta^\beta \quad \text{and} \quad G_e(0) = 0,\ f_e^* = 0,$$

respectively. The trivial solution $f = 0$ also solves (2.9). The linearization of the operator $\mathcal{L}+G_p$ about β^β and $\mathcal{L}+G_e$ about 0 coincide and are equal to $\mathcal{L}+I$, where I is the identity operator. The spectral properties of this non-symmetric operator in a weighted L^2-space play an important part in our analysis and help to describe the perturbation of the solutions from the constant state. They are essential to describe the long time dynamics of both of the PDEs (2.5) and (2.7). We will describe its properties in the next section.

3. Spectral properties of $\mathcal{L}$ and its adjoint.

In this section we study the spectral properties of the linear differential operator $\mathcal{L}$ and it's adjoint $\mathcal{L}^*$ given by

$$\mathcal{L}^* = (-1)^{m+1}D_y^{2m} + \frac{1}{2m}y\frac{d}{dy} + \frac{1}{2m}I. \tag{3.1}$$

Both operators are not symmetric and do not admit a self-adjoint extension. To determine the nature of the stability of the constant solution and also to apply the Fredholm alternative to compute asymptotic solutions of the ODEs, it is necessary to determine the spectrum and corresponding eigenfunctions of both $\mathcal{L}$ and $\mathcal{L}^*$. We present some results from [15] and [20] which describe these.

3.1. The fundamental solution. We start by determining the spectrum and the eigenfunctions of the adjoint operator $\boldsymbol{\mathcal{L}}^*$. In order to find the null eigenfunction, we begin with the fundamental solution of the corresponding linear $2m$th-order parabolic operator. Consider the linear equation

$$u_t = (-1)^{m+1} D_x^{2m} u \quad \text{in } \mathbf{R} \times \mathbf{R}_+. \tag{3.2}$$

The fundamental solution of (3.2) has the standard self-similar form

$$b(x,t) = t^{-1/2m} F(y), \quad y = x/t^{1/2m}. \tag{3.3}$$

Substituting $b(x,t)$ into (3.2) yields that the radially symmetric profile $F(y)$ is the unique even square integrable solution of the linear ODE

$$\boldsymbol{\mathcal{L}}^* F = 0 \quad \text{in } \mathbf{R} \tag{3.4}$$

and is a null eigenfunction of $\boldsymbol{\mathcal{L}}^*$. Taking a Fourier transform leads to

$$F(y) = \alpha \int_0^\infty e^{-s^{2m}} \cos(sy) ds. \tag{3.5}$$

The coefficient α is chosen to normalize $\int F = 1$, so that

$$\alpha = \left(\int_0^\infty \int_0^\infty e^{-s^{2m}} \cos(sy)\, ds\, d\eta \right)^{-1}.$$

The rescaled kernel $F(\eta)$ then satisfies a standard pointwise estimate [16]

$$|F(y)| \le d_1 e^{-d_2 |y|^\nu} \quad \text{in } \mathbf{R},$$

where d_1 and d_2 are positive constants. Applying the Fourier transform to equation (3.2) and performing the rescaling, we have

$$\mathcal{F}(b(\cdot,t))(\xi) = e^{-\xi^{2m} t} \quad \text{and} \quad \hat{F}(\omega) = \mathcal{F}(F(\cdot))(\omega) = e^{-\omega^{2m}}. \tag{3.6}$$

3.2. The discrete real spectrum and eigenfunctions of the adjoint operator $\boldsymbol{\mathcal{L}}^*$. We describe the spectrum $\sigma(\boldsymbol{\mathcal{L}}^*)$ of the adjoint operator in the weighted space $L^2_{\rho^*}(\mathbf{R})$ with the exponential weight

$$\rho^*(y) = e^{a|y|^\nu} > 0 \quad \text{in } \mathbf{R}, \quad \nu = 2m/(2m-1), \tag{3.7}$$

where $a < 2d_2$ is a sufficiently small positive constant. Denoting by $\langle \cdot, \cdot \rangle_*$ and $\| \cdot \|_*$ the corresponding inner product and the induced norm respectively, we introduce a Hilbert space of functions $H^{2m}_{\rho^*}(\mathbf{R})$ with the inner product and the norm

$$\langle v, w \rangle_* = \int_{\mathbf{R}} \rho^*(y) \sum_{k=0}^{2m} D^k v(y)\, \overline{D^k w(y)}\, dy, \quad \|v\|_*^2 = \int_{\mathbf{R}} \rho^*(y) \sum_{k=0}^{2m} |D^k v(y)|^2\, dy.$$

Then $H^{2m}_{\rho^*}(\mathbf{R}) \subset L^2_{\rho^*}(\mathbf{R}) \subset L^2(\mathbf{R})$, and $\boldsymbol{\mathcal{L}}^*$ is a bounded linear operator from $H^{2m}_{\rho^*}(\mathbf{R})$ to $L^2_{\rho^*}(\mathbf{R})$. With these definitions, the spectral properties of the operator $\boldsymbol{\mathcal{L}}$ are given by the following lemma.

Lemma 3.1. *(i) The spectrum of $\boldsymbol{\mathcal{L}}^*$ (and hence of $\boldsymbol{\mathcal{L}}$) comprises real simple eigenvalues only,*

$$\sigma(\boldsymbol{\mathcal{L}}^*) = \{\lambda_k = -k/2m,\ k = 0,1,2,...\}. \tag{3.8}$$

(ii) The eigenfunctions $\psi_k^*(y)$ are given by

$$\psi_k^*(y) = \frac{(-1)^k}{\sqrt{k!}} D^k F(y) \tag{3.9}$$

and form a complete subset in $L^2(\mathbf{R})$ and in $L^2_{\rho^*}(\mathbf{R})$. (Here F is as defined in (3.5).)
(iii) The resolvent $(\boldsymbol{\mathcal{L}}^* - \lambda I)^{-1} : L^2_{\rho^*}(\mathbf{R}) \to L^2_{\rho^*}(\mathbf{R})$ is a compact integral operator.

Most importantly, the operators $\boldsymbol{\mathcal{L}}^*$ and $\boldsymbol{\mathcal{L}}$ have zero Morse index (no eigenvalues have positive real part).

3.3. The polynomial eigenfunctions of the operator $\boldsymbol{\mathcal{L}}$. We now consider the operator (2.6) in the weighted space $L^2_\rho(\mathbf{R})$ ($\langle\cdot,\cdot\rangle$ and $\|\cdot\|$ are the inner product and the norm) with the exponentially decaying weight function

$$\rho(y) \equiv 1/\rho^*(y) = e^{-a|y|^\nu} > 0, \tag{3.10}$$

and ascribe to $\boldsymbol{\mathcal{L}}$ the domain $H^{2m}_\rho(\mathbf{R})$, which is dense in $L^2_\rho(\mathbf{R})$. Then $\boldsymbol{\mathcal{L}}:\ H^{2m}_\rho(\mathbf{R}) \to L^2_\rho(\mathbf{R})$ is a bounded linear operator, $\boldsymbol{\mathcal{L}}^*$ is adjoint to $\boldsymbol{\mathcal{L}}$ and denoting by $\langle\cdot,\cdot\rangle$ the inner product on $L^2(\mathbf{R})$, we have

$$\langle \boldsymbol{\mathcal{L}} v, w\rangle = \langle v, \boldsymbol{\mathcal{L}}^* w\rangle \quad \text{for any } v \in H^{2m}_\rho(\mathbf{R}),\ w \in H^{2m}_{\rho^*}(\mathbf{R}). \tag{3.11}$$

The eigenfunctions of $\boldsymbol{\mathcal{L}}$ take a particularly simple polynomial form and are as follows.

Lemma 3.2. *(i) The eigenfunctions $\psi_k(y)$ of $\boldsymbol{\mathcal{L}}$ are polynomials in y of order k given by*

$$\psi_k(y) = \frac{1}{\sqrt{k!}} \sum_{j=0}^{\lfloor -\lambda_k \rfloor} \frac{(-1)^{mj}}{j!} D^{2mj} y^k, \quad k = 0,1,2,..., \tag{3.12}$$

and form a complete subset in $L^2_\rho(\mathbf{R})$. (Here $\lfloor\cdot\rfloor$ denotes the integer part.)
(ii) $\boldsymbol{\mathcal{L}}$ has compact resolvent $(\boldsymbol{\mathcal{L}} - \lambda I)^{-1}$ in $L^2_\rho(\mathbf{R})$.

Corollary 3.3. *With the definition (3.9) of the adjoint basis, integrating by parts, we have that the orthonormality condition holds*

$$\langle \psi_k, \psi_l^* \rangle = \delta_{k,l} \quad \textit{for any } k,l \ge 0, \tag{3.13}$$

where $\delta_{\kappa,l}$ is the Kronecker delta.

Corollary 3.4. *If $m = 2$, then there are coefficients α_j (depending on k) such that for $k = 4r+2$ and $k = 4r$*

$$\psi_{4r+2} = y^2 \sum_{j=0}^{r} \alpha_j y^{4j} \quad \textit{and} \quad \psi_{4r} = \sum_{j=0}^{r} \alpha_j y^{4j},\ \alpha_0 \ne 0.$$

For example, if $m = 2$ (a case we consider in detail first), then the first four even eigenfunctions are

$$\psi_0(y) = 1, \quad \psi_2(y) = y^2/\sqrt{2}, \quad \psi_4(y) = (y^4 + 24)/\sqrt{24}, \quad \psi_6(y) = y^2(720 + y^4)/\sqrt{6!}, \tag{3.14}$$

with corresponding eigenvalues $0, -1/2, -1, -3/2$.

4. Local asymptotic analysis: invariant subspaces and bifurcation points.

In this section we use the spectral properties of the linearized operators to determine the local stability of the constant solutions of the rescaled PDEs (2.5) and (2.7). We begin with the linearized stability analysis and describe invariant subspaces.

4.1. Invariant eigenspaces. Since nonlinearities under consideration satisfy $G'_p(\beta^\beta) = G'_e(0) = 1$, let us consider solutions of (2.5) and (2.7) as perturbations of the constant solution of the form

$$\theta(y,\tau) = f^* + g(y,\tau) \quad \text{with} \quad \|g\| \ll 1.$$

In both cases g satisfies a perturbed PDE

$$g_\tau = (\boldsymbol{\mathcal{L}} + I)g + \bar{G}(g), \quad \text{where } \bar{G}(g) = G(f^* + g) - g, \tag{4.1}$$

with a quadratic nonlinear perturbation $\bar{G}$

$$\bar{G}(g) = c_2 g^2 + c_3 g^3 + \ldots \quad \text{as} \quad g \to 0, \tag{4.2}$$

and the coefficients depending on the nonlinearity, $c_2 = 1/2$, $c_3 = 1/6$,... for G_e and $c_2 = p(p-1)^{1/(p-1)}/2$, $c_3 = p(p-1)^{2/(p-1)}(p-2)/6$,... for G_p.

In what follows, we restrict our attention to symmetric in x solutions $u = u(|x|,t)$ and hence to symmetric in y rescaled solutions $\theta = \theta(|y|,\tau)$ and $g = g(|y|,\tau)$. In the space $L^2_{0,\rho}(\mathbf{R})$ of symmetric functions, it follows from (3.8), that $\boldsymbol{\mathcal{L}} + I$ has the spectrum

$$\sigma(\boldsymbol{\mathcal{L}} + I) = \{\tilde{\lambda}_k = 1 - k/2m, \ k = 0, 2, 4, \ldots\}. \tag{4.3}$$

Let $\tilde{L}^2_{0,\rho} \subseteq L^2_{0,\rho}$ be the subspace of eigenfunction expansions, where $\{\psi_k\}$ is closed, obtained as the closure of the subset of finite sums $\{v = \sum c_k \psi_k\}$ in the norm $\|\cdot\|$, [15]. Then

$$\tilde{L}^2_{0,\rho}(\mathbf{R}) = E^u(0) \oplus E^c(0) \oplus E^s(0),$$

where $E^u(0)$, $E^c(0)$ and $E^s(0)$ are the unstable, centre and stable subspaces of $\boldsymbol{\mathcal{L}} + I$, given by

$$\begin{aligned} E^u(0) &= \mathrm{Span}\{\psi_0, \psi_2, \ldots, \psi_{2m-2}\}, \\ E^c(0) &= \mathrm{Span}\{\psi_{2m}\}, \\ E^s(0) &= \mathrm{Span}\{\psi_{2m+2}, \ \psi_{2m+4}, \ldots\}. \end{aligned}$$

In particular the dimension of the unstable subspace is precisely m.

Consider the two one-dimensional unstable subspaces corresponding to positive eigenvalues of the operator $\boldsymbol{\mathcal{L}} + I$ namely

$$\tilde{\lambda}_0 = 1, \ \psi_0(y) = 1 \quad \text{and} \quad \tilde{\lambda}_2 = 1 - 1/m, \ \psi_2(y) = y^2/\sqrt{2}. \tag{4.4}$$

As is usual in blow-up problems, the first unstable mode with $k = 0$ corresponds to the instability of blow-up behaviour with respect to perturbations of the blow-up time T.

In contrast, the second mode with $k = 2$ describes an actual instability of the constant solution which is in the direction of $\psi_2(y)$ and is in the space of rescaled solutions having the same fixed blow-up time T. From our asymptotic calculations and numerical experiments we expect that the orbits which arise from the instability of the constant solution in the PDEs (2.7) and (2.5) when $m > 1$ are uniformly bounded and stabilize to one of the self-similar solutions. Namely, the first such unstable mode with $\tilde{\lambda}_2 = 1 - 1/m > 0$ gives a heteroclinic connection of f^* with a non-constant stable (generic) similarity profile $f_1(y)$.

It is significant that when $m = 1$, there is no such unstable mode. In contrast, the dimension of the unstable subspace is one corresponding only to the change in the blow-up time. The eigenfunction ψ_2 then has eigenvalue zero and the behaviour of the perturbations of the constant solution must be studied on the centre manifold. It is this which leads to the approximate self-similar behaviour (1.5) described in the introduction.

Before performing some formal invariant manifold analysis for higher-order PDEs, note that the basic properties of connecting equilibria and transversality of intersections of the corresponding stable and unstable manifolds are known for the one-dimensional second-order parabolic equations

$$u_t = u_{xx} + f(x,u) \quad \text{in } (0,1) \times \mathbf{R}_+, \quad u = 0 \text{ at } x = 0,1 \text{ for } t > 0,$$

and were obtained in [28, 3] and [11] using Sturm's Theorem on the non-increase of the number of zeros (intersections) of solutions to linear second-order parabolic equations. This Sturmian property is not true for the fourth and higher-order parabolic equations (owing to the lack of a maximum principle in these cases) and, in general, the structure of connecting orbits remains an important open problem.

4.2. The centre subspace. Consider the centre subspace $E^c(0)$ in the case of general m. From Lemma 3.2, it follows that the null eigenfunction of the operator $\boldsymbol{\mathcal{L}}$ is given by ψ_{2m} so that

$$\tilde{\lambda}_{2m} = 0 \quad \text{and} \quad \psi_{2m}(y) = [y^{2m} + (-1)^m (2m)!]/\sqrt{(2m)!}\,. \tag{4.5}$$

We now present a simple calculation showing that the behaviour on the centre manifold is semi-stable.

PROPOSITION 4.1. *Let $g(\cdot,\tau) \in H^{2m}_{0,\rho}(\mathbf{R})$ exhibit the centre subspace dominance, i.e.,*

$$g(\cdot,\tau) = a_{2m}(\tau)\psi_{2m}(\cdot) + w(\cdot,\tau) \quad \textit{for } \tau \gg 1, \tag{4.6}$$

where $w(\cdot,\tau) \in \mathcal{L}^{\perp}\{\psi_{2m}\}$ and $w(\cdot,\tau) = o(\|g(\cdot,\tau)\|) = o(|a_{2m}(\tau)|)$ as $\tau \to \infty$. Then

$$a_{2m}(\tau) = -\frac{1}{\gamma_0 \tau}(1 + o(1)) \quad \textit{as } \tau \to \infty, \ \textit{where } \gamma_0 = c_2\langle(\psi_{2m})^2, \psi^*_{2m}\rangle \neq 0. \tag{4.7}$$

It follows from (4.7) that $a_{2m}(\tau)$ cannot change sign in any neighbourhood of $\tau = \infty$ meaning a one-sided instability of the centre manifold behaviour.

Proof. We look for a solution of (4.1) via a uniformly convergent eigenfunction expansion

$$g(\cdot,\tau) = \sum a_k(\tau)\psi_k(\cdot). \tag{4.8}$$

Substituting this expression into (4.1) and multiplying by ψ^*_k in $L^2(\mathbf{R})$, we arrive at a dynamical system for the expansion coefficients

$$\dot{a}_k = \tilde{\lambda}_k a_k + \langle \bar{G}(g), \psi^*_k \rangle, \quad k = 0, 2, \ldots. \tag{4.9}$$

Consider equation for the coefficient a_{2m} with $\tilde{\lambda}_{2m} = 0$. In view of assumption (4.6) and (4.2), assuming that $|a_{2m}(\tau)| \ll 1$, it follows

$$\dot{a}_{2m} = (\gamma_0 + o(1))a_{2m}^2 \quad \text{for } \tau \gg 1. \tag{4.10}$$

Calculating γ_0 by using the adjoint eigenfunction $\psi_{2m}^* = D_y^{2m}F/\sqrt{2m!}$ and (4.5), we obtain that

$$\gamma_0 = c_2(-1)^{m+1}\sqrt{(2m!)}\left(\frac{(4m)!}{[(2m)!]^2} - 2\right). \tag{4.11}$$

Integrating (4.10) as a standard ODE, we deduce that any small solution for $\tau \gg 1$ has the asymptotic behaviour (4.7). □

It follows from the quadratic "ODE" (4.10) that the centre manifold behaviour exhibits a typical semi-stable ("saddle-node") structure. Because the constant profile β^β is only semi-stable, small perturbations in the unstable direction may evolve to self-similar solutions. We present some evidence for this conjecture, and the role of the parity of m in Sections 5 and 6.

In view of known spectral and sectorial properties of operators $\mathcal{L}$ and $\mathcal{L}^*$ [15], [20], we expect that the centre (and stable, see Section 7) manifold behaviour can be justified by the invariant manifold theory in interpolation spaces, see [35], Chapter 9.

4.3. Bifurcation points. In this subsection we extend the ODEs (2.9) and (2.19) for similarity profiles and consider the family of ODEs with a parameter $\mu \geq 0$

$$(-1)^{m+1}D_y^{2m}f - \mu f'y + G(f) = 0 \quad \text{for } y > 0 \text{ with conditions (2.10).} \tag{4.12}$$

Recall that for single-point blow-up, we need to impose an extra condition (of the type (2.16) or (2.22) with $1/2m \mapsto \mu$) on the decay of $f(y)$ at infinity.

If we take $\mu = 1/2m$ and the appropriate nonlinearity, $G = G_p$ or G_e, then we obtain the ODEs (2.9) and (2.19) for the rescaled self-similar profiles. More generally, suitable solutions of (4.12) depend smoothly upon $\mu \approx 1/2m$ and coincide with the self-similar solutions when $\mu = 1/2m$. In either case we define a corresponding linearized operator $\mathcal{L}_\mu$ by

$$\mathcal{L}_\mu = (-1)^{m+1}D_y^{2m} - \mu y D_y + I \equiv \mathcal{L} + (1 - \mu + 1/2m)I. \tag{4.13}$$

Changing the independent variable to

$$y = z/(2m\mu)^{1/2m}, \tag{4.14}$$

we have

$$\frac{1}{2m\mu}\mathcal{L}_\mu = (-1)^{m+1}D_z^{2m} - \frac{1}{2m}z\frac{d}{dz} + \frac{1}{2m\mu}I \equiv \mathcal{L} + \frac{1}{2m\mu}I. \tag{4.15}$$

Hence $\mathcal{L}_\mu : H_{0,\rho}^{2m}(\mathbf{R}) \to L_{0,\rho}^2(\mathbf{R})$ is a bounded linear operator (with a change in the coefficient a in the weight function (3.10) if necessary). By Lemma 3.1, the spectrum $\mathcal{L}_\mu$ in the space $L_{0,\rho}^2(\mathbf{R})$ of radial functions is given by

$$\sigma(\mathcal{L}_\mu) \equiv 2m\mu\,\sigma\left(\mathcal{L} + \frac{1}{2m\mu}I\right) = \{1 - 2\mu l,\ l = 0, 1, 2, ...\}, \tag{4.16}$$

with eigenfunctions ψ_{2l} as before, rescaled according to the transformation (4.14).

We next compute bifurcation points from the constant solution f^*. Since the weight function (3.10) is exponentially decaying as $y \to \infty$, in general, the inclusion $f \in H^{2m}_\rho$ does not imply the boundedness of f unlike the adjoint case of the increasing weight (3.7) where $H^{2m}_\rho \subset C$. Nonlinearity $G(f)$ is not uniformly Lipschitz continuous on bounded subsets from H^{2m}_ρ. Therefore, we truncate the nonlinearity in (4.12) by replacing G by G_n satisfying

$$G_n(f) \equiv G(f) \text{ for } |f| \le n, \;\; n = 1, 2, \,...$$

and $G_n(f)$ is sufficiently smooth and uniformly Lipschitz continuous in $\mathbf{R}$. For $G = G_e$, we need only perform the truncation for $f > n$. We have

$$G_n(f) \to G(f) \quad \text{as } n \to \infty \text{ uniformly on compact subsets.}$$

Replacing the full problem by the truncated one

$$(-1)^{m+1} D_y^{2m} f - \mu y f' + G_n(f) = 0 \tag{4.17}$$

is permissible because we are interested in bounded solutions f for which the nonlinearities $G_p(f)$ and $G_e(f)$ have finite range.

PROPOSITION 4.2. *For any $m \ge 1$, the values of μ for which the spectrum of $\boldsymbol{\mathcal{L}}_\mu$ contains zero,*

$$1 - 2\mu l = 0 \implies \mu_l = 1/2l, \; l = 1, 2, \ldots, \tag{4.18}$$

are bifurcation points for problem (4.17).

Proof. Using rescaling (4.14) and setting $f = f^* + g$, equation (4.17) takes the form

$$(\boldsymbol{\mathcal{L}} - I)g = \tilde{\mu} g + (1 + \tilde{\mu}) G_n(g), \quad \text{where } \tilde{\mu} = -1 - 1/2m\mu. \tag{4.19}$$

Consider the Hammerstein operator $(\boldsymbol{\mathcal{L}} - I)^{-1} G_n$. By Lemma 3.2, $(\boldsymbol{\mathcal{L}} - I)^{-1}$ is a compact operator in $L^2_{0,\rho}$ with simple eigenvalues $\{-1/(1 + l/m) \le -1, \; l = 0, 1, 2, ...\}$. By construction, G_n is uniformly Lipschitz continuous, $|G_n(g)| \le C_1 + C_2 |g|$ in $\mathbf{R}$, and hence $G_n : L^2_{0,\rho} \to L^2_{0,\rho}$. Therefore, the product $(\boldsymbol{\mathcal{L}} - I)^{-1} G_n$ is a compact operator in $L^2_{0,\rho}$, see [33], Chapter V. Hence, in the nonlinear integral equation written as a fixed point problem

$$g = \mathbf{A}(g, \tilde{\mu}) \equiv \tilde{\mu} (\boldsymbol{\mathcal{L}} - I)^{-1} g + (1 + \tilde{\mu}) (\boldsymbol{\mathcal{L}} - I)^{-1} G_n(g), \tag{4.20}$$

bifurcation from the origin occurs iff $\tilde{\mu}$ coincides with characteristic values of $(\boldsymbol{\mathcal{L}} - I)^{-1}$ (simple eigenvalues of $\boldsymbol{\mathcal{L}} - I$), i.e., at $\tilde{\mu}_l = -1 - l/m$ [33]. This yields (4.18). □

Passing to the limit $n \to \infty$, some of the bifurcation sub-branches (which are not of physical interest) may disappear, so that we always need to check which sub-branches are available for $n = \infty$. On the other hand, it is interesting to know for which values of μ, less or greater than μ_l, there exist non-constant solutions and how many. Since the spectrum of the Frechet derivative $\mathbf{A}'(0, \tilde{\mu}_l)$

$$\sigma(\mathbf{A}'(0, \tilde{\mu}_l)) = \{(1 + l/m)/(1 + k/m), \; k = 0, 1, 2, ...\} \tag{4.21}$$

always contains 1 (for $k = l$), the local asymptotic behaviour of bifurcation branches for $\mu \approx \mu_l$ is a delicate problem, and often there exist at least two solutions even in the cases of analytic nonlinearities, see a general theory in [42]. Therefore we will need an extra matching analysis to specify "correct" branches which have the required behaviour at infinity and hence correspond to single-point blow-up similarity profiles.

It is important to mention the main reason for extending the operator (2.6) in (2.9) and (2.19) to the operator in (4.12) parameterized by μ. Setting $\mu = 0$, in the case of the polynomial nonlinearity with $G = G_p$, we recover a well-studied Hamiltonian system, see [2] and the book [38], and the solutions considered in this case can, in principle, be followed as μ increases to the physically important value of $1/2m$. Alternatively, by setting μ close to the bifurcation points (4.18), we can construct asymptotic descriptions of solutions which are local perturbations of the constant solution. This calculation is presented in the next section. Once we have constructed such solutions we may extend again varying μ to determine branches of solutions that persist until the value $\mu_m = 1/2m$.

In other words, problem (4.12) for $\mu \in [0, 1/2m]$ describes the *transition* phenomenon between Hamiltonian systems for $\mu = 0$ with a potential and leading self-adjoint differential operators and the singularity formation problem for $\mu = 1/2m$ with no potential structure or symmetry properties of operators involved.

4.4. Conjecture on existence of self-similar solutions. For any $m > 1$, the questions of the solvability of problem (4.12) for $\mu = 1/2m$ (with the appropriate decay of $f(y)$ at infinity) and of the number of solutions seem to be very hard. Actually, it is a multi-dimensional problem of matching of the $\kappa_m + 1$-dimensional bundle of orbits as $y \to \infty$ (see (2.17)) with the m-dimensional bundle at $y \approx 0$ depending on the parameters $\{f(0), f''(0), ..., f^{(2m-2)}(0)\}$ (a multi-dimensional shooting problem whose complexity increases dramatically as m increases). For $m = 1$, such problem for quasilinear equations (1.3) is well understood in one dimension (see [39] and [8]), though a complete proof of the number, finite or infinite, of solutions for equations in $\mathbf{R}$ and in $\mathbf{R}^N$ is still missing.

We now use the above local bifurcation analysis to estimate the number of solutions from below. In view of Proposition 4.2, there exist branches of solutions $f(y;\mu)$ emanating at $\mu = 1/2l$ from constant solutions $f = f^*$ for each value of $l = 1, ..., m-1$ (though we still do not know which bifurcation branches correspond to single point blow-up profiles with required decay at infinity). In particular, if we fix m, then a self-similar solution occurs at $\mu_m = 1/2m$. However, there are $m - 1$ bifurcation points at $\mu_l = 1/2l > \mu_m = 1/2m$ for $l = 1, ..., m - 1$. The numerical calculations of Section 6 strongly imply that each such bifurcation leads to a branch of solutions $f(y)$ with far-field behaviour of the type (2.16) or (2.22) persisting until μ_m giving rise to a self-similar solution. Furthermore, due to the semi-stability properties of the centre manifold patterns (see further comments in Section 5), we expect from the observations of the previous section, that there is an additional solution of the ODE when m is even. This detail is also supported by both the asymptotic calculations presented in Section 5 and the numerical calculations of Section 6. Combining these observations, let us state the following conjecture suggested by our understanding of the dynamics of the linearized operator, asymptotic constructions and a number of numerical experiments.

CONJECTURE 4.3. *For all $m > 1$, the problems (2.19), and (2.9) have at least $2\lfloor m/2 \rfloor$ (self-similar) solutions.*

Hence, we conjecture that the non-existence of exact self-similar blow-up solutions is a feature only of the second-order semilinear equations, not of all the semilinear equations of the forms (1.6) and (1.7). This conjecture is indeed a lower bound and is based only on properties of the linear operator presented in this paper. In fact, we expect that there are $m(m-1)$ solutions. This estimate is topological and characterizes a typical matching of two multi-dimensional bundles at $y=\infty$ and $y=0$ respectively in the presence of sufficiently strong oscillatory character of the ODE; see further results below.

Further, we note that bifurcations in the limit problem (4.12) hold for arbitrary $L^2_{0,\rho}$-solutions of (4.19), not necessarily satisfying the appropriate decay conditions at infinity. There may also exist non-constant solutions which correspond to stabilization as $y \to \infty$ to another equilibrium,

$$f(y) \to \beta^\beta \text{ for } G = G_p \quad \text{and} \quad f(y) \to 0 \text{ for } G = G_e\,. \tag{4.22}$$

One can see from (2.8) and (2.18) that these self-similar solutions create *global blow-up*, where

$$u(x,t) \to \infty \quad \text{as } t \to T^- \text{ uniformly in } \mathbf{R}. \tag{4.23}$$

Such behaviour is unavailable for $m=1$ as the dimension of the stable manifold about f^* is $2(m-1)$ for m odd. For $m>1$, no such solutions have yet been detected, numerically or otherwise.

5. The asymptotic behaviour of the solutions close to the bifurcation points. In this section we again consider μ to be a continuous parameter in (4.12) and construct an asymptotic description of solutions $f(y;\mu)$ (with the appropriate decay at infinity, see a precise statement below) for μ close to the bifurcation points at $\mu_l = 1/2l$. We set

$$\mu = \mu_l + \sigma_l \varepsilon \quad \text{with } 0<\varepsilon \ll 1 \text{ and } \sigma_l^2 = 1, \tag{5.1}$$

and look for solutions to the ODEs in $\mathbf{R}_+$ for $l = 1,2,\dots$,

$$(-1)^{m+1} f^{(2m)} - (\mu_l + \sigma_l\varepsilon)\, yf' + G_p(f) = 0, \tag{5.2}$$

$$(-1)^{m+1} f^{(2m)} - (\mu_l + \sigma_l\varepsilon)\, yf' + G_e(f) = 0. \tag{5.3}$$

We seek solutions with symmetry conditions (2.10) satisfying the decay condition

$$f(y) = Cy^{-1/(p-1)\mu}(1+o(1)) \quad \text{or} \quad f(y) = -\mu^{-1}\ln y + C + o(1) \quad \text{as } y \to +\infty. \tag{5.4}$$

Here $\sigma_l = \pm 1$ indicates the direction that the branch departs from the constant solution, which we shall show depends upon l and m. Because of the polynomial structure of the eigenfunctions of the linear operator $\boldsymbol{\mathcal{L}}$ (and hence of $\boldsymbol{\mathcal{L}}_\mu$), the asymptotic calculations are similar in spirit for each bifurcation point, $\mu = 1/2l$, although for each order $2m$ of the differential operator there are m slightly different types of expansion. As such we will illustrate the calculations by first considering the case $m=2$ close to arbitrary bifurcation points, then close to the particular bifurcation points of interest to fourth-order PDEs, namely $\mu_1 = 1/2$ and $\mu_2 = 1/4$. Lastly, we construct solutions close to the specific bifurcation points $\mu_m = 1/2m$ for the case of general m to complement the calculations of the centre manifold behaviour described in the previous section and our conjecture regarding the existence of self-similar solutions of the ODE when $\mu = 1/2m$.

5.1. The case of fourth-order ODEs: $m = 2$**.** We shall first consider the two ordinary differential problems, namely finding the slowly growing/bounded solutions of the fourth-order equations with $l = 1, 2, \ldots$,

$$-\,f'''' - (\mu_l + \sigma_l\varepsilon)\,yf' + |f|^{p-1}f - f/(p-1) = 0, \tag{5.5}$$

$$-\,f'''' - (\mu_l + \sigma_l\varepsilon)\,yf' + e^f - 1 = 0. \tag{5.6}$$

The calculation proceeds by identifying three key regions in which asymptotic solutions of three different scalings of the above equations are derived. The three different asymptotic descriptions of the solutions are then matched together. The first region is given by considering solutions for which $\varepsilon^\gamma y$ is small and where

$$\gamma = \begin{cases} \frac{1}{4l} \text{ for } l \text{ odd}, \\ \frac{1}{2l} \text{ for } l \text{ even}. \end{cases} \tag{5.7}$$

Here the solution is near constant and we can express the solution in terms of the eigenfunctions of the linear operator $\boldsymbol{\mathcal{L}}_\mu$ in (4.13). Next is a mid-range region for which $\varepsilon^{-\gamma} < y < e^{1/\varepsilon}$ where the appropriately rescaled differential equations reduce to an integrable first order equation. Lastly, there is the region $\{y > e^{1/\varepsilon}\}$ where the solution satisfies the far-field behaviour (5.4).

5.1.1. The behaviour of $f(y)$ **for** $\varepsilon^\gamma y \ll 1$**.** We begin by seeking solutions to (5.5) and (5.6) which are valid for small $\varepsilon^\gamma |y|$ and which are close to the constant solutions of the respective nonlinearities. Consider the corresponding equation (4.20) for fixed points. Since by (4.21), 1 is an eigenvalue of $\mathbf{A}'(0, \tilde{\mu}_l)$ with the one-dimensional eigenspace E_l, according to the general branching theory [42], Chapter 5, in this special case we seek solutions of the form of the rational series

$$f(y) = f_0 + \varepsilon^q f_1(y) + \varepsilon^{2q} f_2(y) + \ldots \tag{5.8}$$

where we denote $f_0 = f^*$. For convenience, we perform this equivalent expansion analysis directly for the ODEs and avoid using the integral equation (4.20) with compact operators. The exponent $q = 1/n$ with an unknown integer $n \geq 1$ is to be determined from the solvability of the corresponding nonlinear systems on the expansion coefficients (the branching equation). Since dim $E_l = 1$, the branching equation is always one-dimensional. Note that for analytic nonlinearities, i.e., equation (5.6) with any odd p and (5.5), in the case of one (or two) dimensional eigenspace E_l, finite solvability of such systems (existence of a finite number of solutions) implies convergence of the series (5.8) for sufficiently small ε, although we can expect there to be at least two different bifurcating branches of solutions, see [42], pp. 209-211. We then determine the correct branch by matching to solutions with the appropriate decay properties at infinity.

The rational power q of the order parameter depends on the coefficients of the branching equation which are different depending on whether l is even or odd. Substituting the expansion (5.8) into the ODEs leads, at lowest order, to an ODE for $f_1(y)$ of the form

$$\boldsymbol{\mathcal{L}}_{1/2l} f_1 \equiv -f_1'''' - \frac{1}{2l} y f_1' + f_1 = 0.$$

Accordingly, the leading order approximation to $f - f_0$ is given by a linear multiple of the eigenfunction $\psi_{2l}((2/l)^{1/4} y)$, see (4.14). From the description of the spectrum of the operator $\mathcal{L}$ given in Lemma 3.1, using Corollary 3.2, we know that (as $m = 2$) the transformed operator $\mathcal{L}_{1/2l}$ has null eigenfunctions ψ_{2l} which are polynomials and which take the form

$$\psi_{2l}(y) = y^2 \sum_{j=0}^{(l-1)/2} \alpha_j y^{4j} \;\text{ for } l \text{ odd} \quad \text{and} \quad \psi_{2l}(y) = \sum_{j=0}^{l/2} \alpha_j y^{4j} \;\text{ for } l \text{ even},$$

as defined by (3.12) after the change of variable $y \mapsto y(2/l)^{1/4}$.

The difference between the cases of l even and l odd is as follows. In the asymptotic expansion, the higher powers of $f_1(y)$ become forcing terms to equations involving the operator $\mathcal{L}_{1/2l} f_j$. In the case of odd l these terms will always be polynomials in y^4. These may have no contribution which resonates with the null eigenfunction ψ_{2l} of $\mathcal{L}$. In contrast, the powers of $f_1(y)$ for even l will always have contributions which resonate with $\psi_{2l}(y)$. As a consequence, the cases l even and l odd lead to distinctly different forms of asymptotic expansion, in particular, $q = 1/2$ for odd l and $q = 1$ for even l. In other words, for l even and odd the branching equation changes its type. Generically, there will be m distinct expansions in powers of $\varepsilon^{i/m}$, $i = 1, 2, ..., m$, see a general classification in [42], Section 12.

A The case of $m = 2$ and l odd. We take $l = 2r + 1$ so that the bifurcation point is at $\mu = 1/(4r + 2)$, $r = 0, 1, \ldots$. We express $f(y)$ as an asymptotic expansion ($q = 1/2$)

$$f = f_0 + \varepsilon^{1/2} f_1 + \varepsilon f_2 + \varepsilon^{3/2} f_3 + \ldots \ . \tag{5.9}$$

This expansion corresponds to the case of branching equation described in Theorem 12.2 in [42], where there exist two solutions either for $\mu < \mu_l$ or for $\mu > \mu_l$. Substituting the expansion (5.9) into either equation (5.5) or (5.6) gives a sequence of ODE problems of the form

$$\begin{aligned}
&O(\varepsilon^{1/2}): \quad && \mathcal{L}_{1/2l} f_1 \equiv -f_1'''' - \frac{1}{4r+2} y f_1' + f_1 = 0, && (5.10)\\
&O(\varepsilon): && \mathcal{L}_{1/2l} f_2 = -c_2 f_1^2, && (5.11)\\
&O(\varepsilon^{3/2}): && \mathcal{L}_{1/2l} f_3 = \sigma_l y f_1' - 2c_2 f_1 f_2 - c_3 f_1^3, \ \ldots, && (5.12)
\end{aligned}$$

where $c_2, c_3, ...$ are as given in (4.2). In each case we seek solutions from $H^{0,2m}_\rho(\mathbf{R})$. In view of asymptotic properties for linearized operators in Section 2, the solutions are assumed to grow slowly (at worst polynomially) as y increases and which will ultimately be matched to solutions of the ODEs (5.2) and (5.3) which have the correct behaviour at infinity, (5.4).

As observed above, it follows from (4.16) that the lowest order equation (5.10) can be solved in terms of a rescaling of the null eigenfunction ψ_{2l} of $\mathcal{L}_{2l}$. Applying in (3.12) the scaling $y \mapsto (2/(2r+1))^{1/4} y$, it follows that there is a constant α such that

$$f_1(y) = \alpha \tilde{f}_1(y), \quad \text{where } \tilde{f}_1(y) = \sum_{j=0}^{r} \left(\frac{(2r+1)}{2}\right)^{j-r-1/2} \frac{1}{j!} D^{4j} y^{4r+2}. \tag{5.13}$$

For example, $f_1(y) = \alpha y^2$ when $r = 0$ and $\mu = 1/2$. Here the constant α is unspecified at this level of expansion and will be determined by a solvability condition for the higher order terms.

The Fredholm alternative gives the orthogonality condition for the second equation (5.11) at order ε to have a solution in $H^{2m}_{0,\rho}(\mathbf{R})$,

$$\langle f_1^2, \psi_{2l}^* \rangle = 0, \tag{5.14}$$

where $\psi_{2l}^* = \psi_{2l}^*((2/l)^{1/4}y)$ defined in (3.9) is the eigenfunction of the adjoint operator $\boldsymbol{\mathcal{L}}^*_{1/2l}$. If $r = 0$ and $l = 1$, then the first three even eigenfunctions of $\boldsymbol{\mathcal{L}}_{1/2}$ are given in (3.14). Since ψ_2^* is the null eigenfunction of $\boldsymbol{\mathcal{L}}^*_{1/2l}$, it follows that $\langle \psi_2^*, \psi_0 \rangle = 0$ and $\langle \psi_2^*, \psi_4 \rangle = 0$. Hence $\langle \psi_2^*, y^4 \rangle = \langle \psi_1, f_1^2 \rangle = 0$, so that the orthogonality (5.14) holds and there exists solutions of equation (5.11) at this order. This is the lack of resonance condition that we described earlier.

For arbitrary r, by (5.13),

$$f_1^2(y) = \alpha^2 \sum_{j=0}^{2r} a_j y^{4j+4},$$

and we find a particular polynomial solution of (5.11) in the form

$$\alpha^2 \tilde{f}_2(y) = -c_2 \alpha^2 \sum_{j=-1}^{2r} b_j y^{4j+4}. \tag{5.15}$$

Substituting it into the equation and equating the coefficients gives

$$b_{2r} = -a_{2r}, \quad b_{-1} = 4!\, b_0 \quad \text{and} \tag{5.16}$$

$$b_j = \frac{2r+1}{2(r-j)-1} \left[a_j + b_{j+1} \frac{(8+4j)!}{(4+4j)!} \right] \quad \text{for } j = 2r-1, \ldots, 0. \tag{5.17}$$

Hence, the orthogonality condition (5.14) holds. The general solution of (5.11) is given by

$$f_2(y) = \alpha^2 \tilde{f}_2(y) + \alpha_1 \tilde{f}_1(y), \tag{5.18}$$

where α_1 is an extra real unknown.

The unknowns α and α_1 are determined by applying the Fredholm alternative at the next orders of expansion. In equation (5.12), similar to (5.14), the solvability condition is given by

$$\left\langle \sigma_l y f_1' - 2c_2 f_1 f_2 - c_3 f_1^3, \psi_{2l}^* \right\rangle = 0. \tag{5.19}$$

Substituting (5.13) and (5.18) yields the algebraic equation

$$\alpha A - \alpha^3 B + \alpha \alpha_1 C = 0, \tag{5.20}$$

where $A = \langle \sigma_l y f_1', \psi_{2l}^* \rangle$, $B = \langle c_3 \tilde{f}_1^3 + 2c_2 \tilde{f}_1 \tilde{f}_2, \psi_{2l}^* \rangle$ and the third coefficient C vanishes by the first solvability criterion (5.14),

$$C = -2C_2 \langle \tilde{f}_1^2, \psi_{2l}^* \rangle = 0. \tag{5.21}$$

Equation (5.20) is a cubic equation for the first unknown α only, $\alpha(\alpha^2 - \sigma_l \gamma) = 0$, where γ can be computed explicitly. The $\alpha = 0$ case simply corresponds to the constant solution (the trivial expansion (5.9)) and can be discarded. Hence, we have two solutions

$$\alpha = \pm\sqrt{\sigma_l \gamma}\,. \tag{5.22}$$

The sign of σ_l is thus the same as that of γ while the sign of α follows from matching to the far field solution (see Section 5.2). In general, the second unknown α_1 (together with an extra one α_3 obtained from the homogeneous equation (5.12), etc.) is to be determined from the solvability conditions of equations for the coefficients f_4, f_5,... of higher-order perturbations. Although not presented, higher approximations follow in a similar manner to those here.

Example. To illustrate this calculation, we now look at the two cases of $l = 1$ and $l = 3$ for the quadratic nonlinearity with $p = 2$, where $G_p(f) = |f|f - f$. These are chosen so that the corresponding bifurcation points at $\mu = 1/2$ and $\mu = 1/6$ are either side of the "self-similar" value of $\mu_2 = 1/4$.

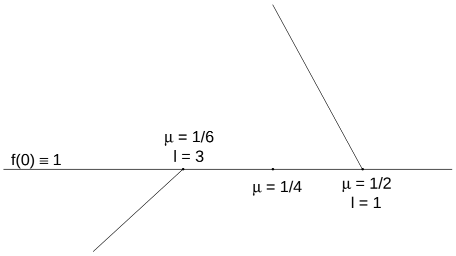

FIG. 5.1. *Sketch of the bifurcation points under consideration.*

THE FIRST BIFURCATION POINT: $\mu_1 = 1/2$ $(l = 1,\ r = 0)$. As observed above, when $l = 1$ we have $f_0 = 1$ and $f_1 = \alpha y^2$. A simple calculation then gives $f_2 = \alpha^2(y^4 + 24)$ and expansion (5.9) takes the form

$$f(y) = 1 + \alpha\varepsilon^{1/2} y^2 + \varepsilon\left[\alpha^2(y^4 + 24) + \alpha_1 y^2\right] + \varepsilon^{3/2} f_3(y) + \dots\,. \tag{5.23}$$

Observe that since $c_3 = 0$, the solvability condition (5.19) for f_3 is then given by

$$\langle 2\sigma_1 \alpha y^2 - 2\alpha^3 y^2 (y^4 + 24), \psi_2^* \rangle = 0, \quad \psi_2^* = \psi_2^*(2^{1/4} y). \tag{5.24}$$

To calculate α, we exploit the fact that $\hat{\psi}_2^*(\omega) = -\omega^2 e^{-\omega^4}/\sqrt{2}$ by (3.6) and (3.9). Recall also that if a function $f(y)$ has Fourier transform $\hat{f}(\omega)$, then

$$\langle f, y^{2n} \rangle = (-1)^n \hat{f}^{(2n)}(0). \tag{5.25}$$

Taking $\psi_2^* = \psi_2^*(2^{1/4} y)$ yields $\langle \psi_2^*(2^{1/4} y), y^2 \rangle = 1/2^{1/4}$, $\langle \psi_2^*(2^{1/4} y), y^6 \rangle = -180/2^{1/4}$, the solvability condition (5.24) reduces to the cubic equation $\sigma_1 \alpha + 156\alpha^3 = 0$ and hence

$$\sigma_1 = -1 \quad \text{and} \quad \alpha = \pm\frac{1}{\sqrt{156}} = \pm\frac{\sqrt{39}}{78}, \tag{5.26}$$

so that (5.23) yields

$$f(y) = 1 \pm \varepsilon^{1/2} \frac{y^2}{\sqrt{156}} + \varepsilon\left(\frac{1}{156}(y^4 + 24) + \alpha_1 y^2\right) + \dots\,. \tag{5.27}$$

The sign of α will be determined by matching to the solution in the mid-range. We show presently that $\alpha < 0$ so that

$$f(y) = 1 - \varepsilon^{1/2}\frac{y^2}{\sqrt{156}} + \varepsilon\left(\frac{1}{156}(y^4 + 24) + \alpha_1 y^2\right) + \ldots$$

and, in particular, since $\varepsilon > 0$,

$$f(0) = 1 + 2\varepsilon/13 + \ldots > 1. \tag{5.28}$$

The resulting branch thus bifurcates to the left, and exists locally only for $\mu < 1/2$, there is no possible matching to a decaying solution for $\mu > 1/2$. The numerical calculations reported in the next section indicate that the branch persists globally, so that solutions exist at the self-similar value $\mu_2 = 1/4$.

THE THIRD BIFURCATION POINT: $\mu_l = 1/6$ $(l = 3,\ r = 1)$. We again have $f_0 = 1$ and now $f_1(y) = \alpha(y^6 + 540y^2)$ and $f_2 = \alpha^2(y^{12} - 32400y^8 - 164170800y^4 - 3940099200)$, so that the expansion is

$$\begin{aligned} f = {} & 1 + \varepsilon^{1/2}\alpha\left(y^6 + 540y^2\right) \\ & + \varepsilon\left(\alpha^2\left(y^{12} - 32400y^8 - 164170800y^4 - 3940099200\right) + \alpha_1\tilde{f}_1\right) + \ldots . \end{aligned}$$

A similar (but much longer) analysis of the orthogonality condition (5.19) with eigenfunction $\psi_6((2/3)^{1/4}y) = (y^6 + 540y^2)/12\sqrt{5}$ then indicates that the branch again bifurcates to the left and exists locally for $\mu < 1/6$.

B THE CASE OF $m = 2$ AND l EVEN. In the case $l = 2r$ the bifurcation occurs at the point $\mu_{2r} = 1/4r$. Because of the presence of a constant term in the eigenfunction ψ_{2l}, the effect of the "forcing terms" yf' comes in at lower order than in the previous case. This leads to a standard asymptotic expansion for $f(y)$ of the form (cf. Theorem 12.1 in [42])

$$f = f_0 + \varepsilon f_1 + \varepsilon^2 f_2 + \ldots . \tag{5.29}$$

Substituting this expression for f into (5.5) or (5.6) gives

$$O(\varepsilon): \quad \mathcal{L}_{1/2l} f_1 \equiv -f_1'''' - \frac{1}{4r} y f_1' + f_1 = 0, \tag{5.30}$$

$$O(\varepsilon^2): \quad \mathcal{L}_{1/2l} f_2 = \sigma_l y f_1' - c_2 f_1^2. \tag{5.31}$$

As before, we express f_1 as a multiple of the (scaled) eigenfunction $\psi_{2l}(r^{-1/4}y)$,

$$f_1(y) = \alpha\tilde{f}_1(y) \equiv \alpha \sum_{j=0}^{r} \frac{r^{j-r}}{j!} D^{4j} y^{4r}. \tag{5.32}$$

The value of α is determined by considering the solvability condition for equation (5.31) at $O(\varepsilon^2)$. From the analysis above, it follows that for f_2 to exist we must have

$$\langle \sigma_l y f_1' - c_2 f_1^2, \psi_{2l}^* \rangle = 0 \quad \text{with } \psi_{2l}^* = \psi_{2l}^*((2/l)^{1/4}y). \tag{5.33}$$

This leads to a quadratic equation in α of the form $\alpha(\alpha - \gamma) = 0$, where γ may again be determined explicitly. This is the case of a unique nontrivial solution existing for both $\mu > \mu_l$ and $\mu < \mu_l$, and again we will need an extra matching argument to determine the correct sub-branch.

To illustrate this calculation, we again take $p = 2$, $G_p(f) = |f|f - f$ and now consider the case of $l = 2$. This is an especially important value as it corresponds to $\mu_2 = 1/4$ at which the self-similar solution exists. In this case we have $f_0 = 1$ and $f_1 = \alpha(y^4 + 24)$. The solvability condition for α is now

$$\langle \sigma_2 y f_1' - f_1^2, \psi_4^*(y)\rangle = \langle 4\sigma_2\alpha y^4 - \alpha^2(y^4+24)^2, \psi_4^*(y)\rangle = 0.$$

We have that $\hat{\psi}_4^*(\omega) = \omega^4 e^{-\omega^4}/2\sqrt{6}$ and it follows that the quadratic equation satisfied by α is given by

$$96\sigma_2\alpha + 39168\alpha^2 = 0 \quad \Longrightarrow \quad \alpha = -\sigma_2/408. \tag{5.34}$$

We show presently that to match with the mid-range, we have to have $\alpha < 0$ so that $\sigma_2 = 1$. Hence

$$f(y) = 1 - \frac{\varepsilon}{408}\left(y^4 + 24\right) + \varepsilon^2\left[\tilde{f}_2(y) + \alpha_1 \tilde{f}_1(y)\right] \dots, \tag{5.35}$$

where the third term (actually we do not need to compute it) explains the spatial non-monotonicity of such a solution. If $\varepsilon > 0$, then

$$f(0) = 1 - \varepsilon/17 + O(\varepsilon^2) < 1. \tag{5.36}$$

5.1.2. The mid-range $\varepsilon^\gamma < y < e^{1/\varepsilon}$. The mid-range behaviour is governed by the solutions of a first-order equation, which is different for each nonlinearity. However, the calculation now takes the same form for both l even and odd and uses a regular asymptotic expansion. To study the mid-range, we rescale the underlying ODEs in space according to the transformation

$$s = \varepsilon^\gamma y \geq 0 \qquad (\gamma \text{ as in } (5.7)). \tag{5.37}$$

The outer limit of the inner region can be matched to the mid-range region by taking s to be small and y to be large.

A THE CASE $G_p(f) = |f|^{p-1}f - f/(p-1)$. Under the spatial rescaling (5.37), equation (5.5) becomes

$$-\varepsilon^{4\gamma} f'''' - (\mu_l + \sigma_l \varepsilon)\, s f' + |f|^{p-1} f - f/(p-1) = 0, \quad l = 1, 2, \dots, \tag{5.38}$$

where $' = d/ds$. To solve this, we pose a regular asymptotic expansion

$$f = f_0 + \varepsilon^{4\gamma} f_1 + \varepsilon^{8\gamma} f_2 + \dots. \tag{5.39}$$

To leading order we have simply the first-order ODE $-yf_0'/2l + |f_0|^{p-1}f_0 - f_0/(p-1) = 0$, which has a family of bounded positive exact solutions

$$f_0(s) = [(p-1) + \kappa s^{2l}]^{-1/(p-1)}, \tag{5.40}$$

where $\kappa > 0$ is a positive constant.

Note that for *small* s, we have

$$f_0(s) = \beta^\beta \left(1 - \frac{\kappa}{(p-1)^2} s^{2l} + \frac{p\kappa^2}{2(p-1)^4} s^{4l} + O(s^{8l})\right), \tag{5.41}$$

whilst for *large s*

$$f_0(s) = \kappa^{-1/(p-1)} s^{-2l/(p-1)} + \dots . \tag{5.42}$$

We now consider the next term in the asymptotic expansion, looking at the two cases of small s and large s separately. The function f_1 satisfies the equation

$$-\frac{1}{2l} s f_1' + \left[\frac{p}{(p-1) + \kappa s^{2l}} - \frac{1}{(p-1)} \right] f_1 = \sigma_l s f_0' + f_0'''' .$$

We consider for simplicity the case of $p = 2$, and look at the three cases of $l = 1, 2$ and 3.

If $l = 1$, then $4\gamma = 1$ and for small s, we have $f_0(s) = 1 - \kappa s^2 + \frac{1}{2}\kappa^2 s^4 + \dots$, thus the leading order contribution to $\sigma_l s f_0' + f_0''''$ is simply $12\kappa^2$ and hence we have, to leading order as $s \to 0$,

$$f_1(s) = 12\kappa^2 + \dots .$$

If $l = 2$, then $4\gamma = 1$ and for small s, $f_0(s) = 1 - \kappa s^4 + \frac{1}{2}\kappa^2 s^8 + \dots$ so that, to leading order

$$f_1(s) = -24\kappa + \dots .$$

If $l = 3$, then $4\gamma = 1/3$ and for small s, $f_0(s) = 1 - \kappa s^6 + \frac{1}{2}\kappa^2 s^{12} + \dots$ so that, to leading order $f_0'''' = -360\kappa s^2$ and

$$f_1(s) = -540\kappa s^2 + \dots .$$

We conclude that the small s limit of the mid-range solution is

$$f = 1 - \kappa s^2 + \kappa^2 s^4/2 + \dots + \varepsilon(12\kappa^2 + \dots), \quad \text{if} \quad l = 1, \tag{5.43}$$

$$f = 1 - \kappa s^4 + \kappa^2 s^8/2 + \dots - \varepsilon(24\kappa + \dots), \quad \text{if} \quad l = 2, \tag{5.44}$$

$$f = 1 - \kappa s^6 + \kappa^2 s^{12}/2 + \dots - \varepsilon(540\kappa^2 s^2 + \dots), \quad \text{if} \quad l = 3. \tag{5.45}$$

In terms of the original variable y we have

$$f = 1 - \varepsilon^{1/2}\kappa y^2 + \varepsilon\kappa^2(y^4/2 + 12) + \dots , \quad \text{if} \quad l = 1, \tag{5.46}$$

$$f = 1 - \varepsilon\kappa(y^4 + 24) + \varepsilon^2\kappa^2 y^8/2 + \dots , \quad \text{if} \quad l = 2, \tag{5.47}$$

$$f = 1 - \varepsilon^{1/2}\kappa(y^6 + 540y^2) + \varepsilon\kappa^2 y^{12}/2 + \dots , \quad \text{if} \quad l = 3. \tag{5.48}$$

We can now consider matching the above expressions to the expansions given in the last sections.

If $l = 1$, then comparing with (5.27) we have a perfect match provided that $\kappa = -\alpha$. As $\kappa > 0$, it follows that $\alpha = -1/\sqrt{156}$. Thus, in the mid-range when $l = 1$ we have

$$f_0(y) = (1 + \varepsilon^{1/2} y^2/\sqrt{156})^{-1}.$$

As remarked earlier, this bifurcation branch exists only if $\mu < 1/2$.
If $l = 2$, then comparing with (5.35), we again have a perfect match if $\kappa = -\alpha > 0$. In the mid-range when $l = 2$ there holds

$$f_0(y) = (1 + \varepsilon^{1/2} y^4/408)^{-1}.$$

Note, that this expression is only meaningful if $\epsilon > 0$. As in this case $\sigma_2 = 1$, it follows that locally the branch of solutions which bifurcates from $\mu = 1/4$ exists only if $\mu > 1/4$. Numerically we observe that this curve continues globally for values of $\mu < 1/4$ and hence there is a fold bifurcation at some point $\mu = \mu_* > 1/4$, with a *non-zero* solution on the branch existing at $\mu = 1/4$. This corresponds to a self-similar solution distinct from that lying on the branch bifurcating from the point $\mu = 1/2$. The existence of such a solution is consistent with the semi-stability of the centre manifold determined in Section 4.
If $l = 3$, then comparing with the inner expansion, we again have a match if $\kappa = -\alpha > 0$ and in the mid-range

$$f_0(y) = (1 - \alpha\varepsilon^{1/2}y^6)^{-1} \quad (\alpha < 0).$$

Now consider the behaviour for $s \gg 1$ when $p = 2$. For these values of s, to leading order, the function f_1 satisfies the ODE $-\mu_l s f_1' - f_1 = -2l\sigma_l/\kappa s^{2l} + \dots$, hence,

$$f_1(s) = 4l^2\sigma_l \ln s/\kappa s^{2l} + \dots \quad \text{as } s \to \infty\,.$$

Or, returning to the original variable y,

$$f(y) = \frac{1}{\kappa\varepsilon^{l/2}y^{2l}}\left(1 + 4l^2\sigma_l \ln y + \dots\right) \quad \text{as} \quad y \to \infty. \tag{5.49}$$

B *The case of* $G = e^f - 1$. Under the same spatial rescaling as before, the equation (5.6) becomes

$$-\varepsilon f'''' - (\mu_l + \sigma_l\varepsilon)\, sf' + e^f - 1 = 0, \quad l = 1, 2, \dots\,.$$

Posing expansion (5.39), substituting into the ODE and solving the leading order equation gives

$$f_0(s) = -\ln(1 + \kappa s^{2l}). \tag{5.50}$$

The analysis now proceeds as above, and again matching in the limit $s \to 0$ fixes $\kappa > 0$.

5.1.3. Far field behaviour.

The correct far field behaviour is determined by assuming slow growth in both (5.2) and (5.3), $f''''(y) \to 0$ as $y \to \infty$ and hence $|f|f \ll f$ for small $f > 0$ there in (5.5), while $e^f \ll 1$ for $f \ll -1$ in (5.6). In the case of (5.5), this gives

$$f = Cy^{-1/\mu}(1 + o(1)) \equiv Cy^{-2l/(1+2l\sigma_l\varepsilon)}(1 + o(1)) \quad \text{as } y \to \infty.$$

Expanding this for $\varepsilon \ll 1$, we have

$$f = Cy^{-2l}(1 + 4l^2\sigma_l\varepsilon \ln y) + \dots \quad (\varepsilon|\ln y| \ll 1).$$

This matches with (5.49) if $C = 1/\kappa\varepsilon^{l/2}$ (note that $\kappa = |\alpha|/\varepsilon$ for $l = 3$).

5.2. Bifurcations from $\mu_m = 1/2m$ for general m.

As remarked, for $m = 2$ we can also postulate existence of the new profile f_2 from the shape of the branch associated with $\mu_2 = 1/4$ as the branch leaves the bifurcation point to the right and then is expected to fold back. In fact, this behaviour can be understood for general m.

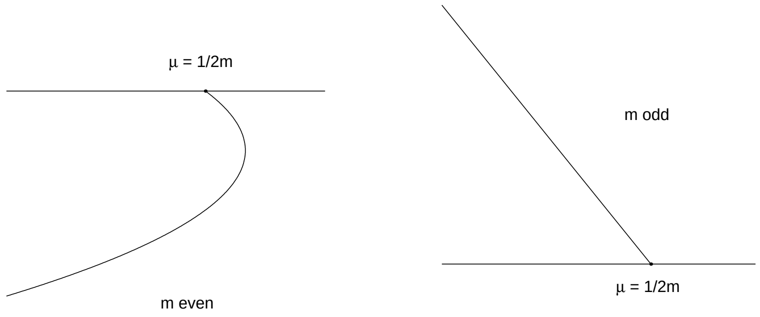

FIG. 5.2. *Schematic of the distinction between even and odd m.*

For all m, the bifurcation point $\mu_m = 1/2m$ is associated with a zero eigenvalue of the linearized operator $\boldsymbol{\mathcal{L}} + I$ in the PDE (4.1). Further evidence for the existence of a nonlinear pattern associated with this point comes from the local structure of the bifurcation diagram. Looking for small solutions near this point, we solve

$$(-1)^{m+1} D_y^{2m} f - \mu_m y D_y f + f + \sigma_m \varepsilon y D_y f + \bar{G}(f - f_0) = 0,$$

where $\bar{G}$ is the quadratic perturbation (4.2). At $\mu_m = 1/2m$ we have the regular expansion (5.29) and expanding as before gives

$$\mathcal{L}_{1/2m} f_1 = 0 \quad \Longrightarrow \quad f_1 = \alpha \left[y^{2m} + (-1)^m (2m)! \right] \quad \text{with unknown } \alpha \in \mathbf{R}.$$

At the next order we have

$$\mathcal{L}_{1/2m} f_2 = \sigma_m y f_1' - c_2 f_1^2 = 2m\sigma_m \alpha y^{2m} - c_2 \alpha^2 \left([(2m)!]^2 + 2(-1)^m (2m)! y^{2m} + y^{4m} \right). \tag{5.51}$$

By the Fredholm alternative this can be solved only if

$$\left\langle 2m\sigma_m \alpha y^{2m} - c_2\alpha^2 \left([(2m)!]^2 + 2(-1)^m (2m)! y^{2m} + y^{4m} \right), \psi_{2m}^*(y) \right\rangle = 0.$$

By (3.9) $\hat{\psi}_{2m}^*(\omega) = \omega^{2m} e^{-2m} / \sqrt{(2m)!}$ so that, after a little manipulation noting that

$$\langle 1, \psi_{2m}^* \rangle = 0, \quad \langle y^{2m}, \psi_{2m}^* \rangle = (2m)!, \quad \langle y^{4m}, \psi_{2m}^* \rangle = (-1)^{m+1} (2m)!,$$

the solvability condition becomes

$$2m\sigma_m \alpha (2m)! - c_2 \alpha^2 (-1)^{m+1} \left((4m)! - 2[(2m)!]^2 \right) = 0.$$

Thus, the solvability condition implies that

$$\alpha = (-1)^{m+1} \frac{\sigma_m}{c_2} \frac{2m(2m)!}{(4m)! - 2[(2m)!]^2} \tag{5.52}$$

and hence

$$f(y) = f_0 + (-1)^{m+1} \varepsilon \frac{\sigma_m}{c_2} \frac{2m(2m)!}{(4m)! - 2[(2m)!]^2} \left(y^{2m} + (-1)^m (2m)! \right) + \ldots .$$

But, to match with the mid-range, we require that $f_1 \to -\infty$ as $y \to \infty$, i.e., $\alpha < 0$ in (5.52), which sets

$$\sigma_m = (-1)^m \quad \text{for} \quad \varepsilon > 0.$$

Hence, by (5.1) for even m, the branches initially increase in μ and thus, if they have folded back, contribute an extra similarity profile $f_m(y)$ at $\mu = 1/2m$, whereas there need be no such contribution for odd m.

The existence of a *second* self-similar solution in the case $m = 2$ to the ODE is suggested by the center manifold analysis in Proposition 4.1. More precisely, consider the *unstable* centre manifold behaviour (4.6) for any even m

$$g(y,\tau) = -\frac{1}{\gamma_0 \tau}\psi_{2m}(y) + \ldots \to 0 \quad \text{as } \tau \to -\infty, \tag{5.53}$$

where $\psi_{2m} > 0$ is given by (4.5). We suppose that $g(\cdot,\tau)$ becomes sufficiently large as $\tau \approx -0$. Hence, $g(y,\tau) < 0$ for $\tau \ll -1$ on any compact subset in y, i.e., the corresponding solution of the PDE (2.5) (or (2.7)) satisfies $\theta(y,\tau) = \beta^\beta + g(y,\tau) < \beta^\beta$. Such a solution can be extended as above to satisfy $\theta(y,\tau) \to 0$ as $y \to \infty$, see also [20]. This shows that such an orbit cannot be a heteroclinic connection $\beta^\beta \to 0$, since for $\tau \approx -0$ this would mean that $|\theta(y,\tau)|$ gets essentially smaller than the constant blow-up profile β^β. Hence $\theta(y,\tau)$ cannot correspond to a solution $u(x,t)$ of the PDE which blows up at the fixed $t = T$; see L^∞-estimates of the blow-up rate in [10] and [21]. Therefore, this $\theta(\cdot,\tau)$ can be assumed to describe an orbital connection $\beta^\beta \to f_m(y)$ to a new nontrivial similarity profile f_m existing at $\mu = \mu_m$. Note that by construction, it is expected that a certain approximated order occurs meaning that $f_m(y) \lesssim \beta^\beta$ in $\mathbf{R}$ in a natural sense.

On the other hand, for odd m's, $\psi_{2m}(y)$ in (4.5) changes sign and we do not have such a contradiction (one can see that an orbital connection $\beta^\beta \to 0$ is possible, see such a centre manifold pattern in [24]).

6. Numerical calculations of the self-similar profiles. We next present a numerical calculation of the solutions of the problem (4.12) parameterized by μ and taking $G_p(f) = |f|f - f$ for $p = 2$ (as indicated from the analysis of the previous sections, the case $G_e(f) = e^f - 1$ is fundamentally the same and is omitted for the sake of brevity). This calculation allows us to extend the asymptotic analysis of the previous section, and, in particular, to study the global behaviour of the branches which bifurcate from the first two bifurcation points at $\mu_1 = 1/2$ and $\mu_2 = 1/4$. The solutions were obtained using a collocation code which guarantees a small residual tolerance [40]. The initial points on each curve were obtained by setting $\mu = 0$. The continuation of each solution was then done by using the pseudo arc-length routine in AUTO [13]. Symmetry conditions were imposed at the origin and minimal growth was enforced at the far field by solving the problem on the finite interval $(0, 1000)$ and setting the highest derivatives to zero at the right-hand boundary.

6.1. The fourth-order case $m = 2$. In Figure 6.1 we present the results of the numerical calculations for different values of the parameter μ looking at the fourth-order differential equations given by taking $m = 2$. In this figure we use $f(0)$ as a measure of the size of the solution. The existence of branches bifurcating from each of the points $\mu_l = 1/2l$ (displayed as solid lines) is clear. Also plotted in dashed lines are other solutions obtained from continuing solutions from $\mu = 0$ which do not bifurcate from the constant solution $f \equiv 1$. In this format it is difficult to distinguish the solutions which bifurcate from the linear spectrum from the additional "nonlinear" solutions. To make this distinction clear we plot the same solutions in Figure 6.2 using the L^2_ρ-norm as the solution measure.

We observe firstly that the curve bifurcating from $\mu_1 = 1/2$ appears to exist for all values of $\mu \in [0, 1/2]$ and, in particular, there is a non-constant solution $f_s(y)$ (the

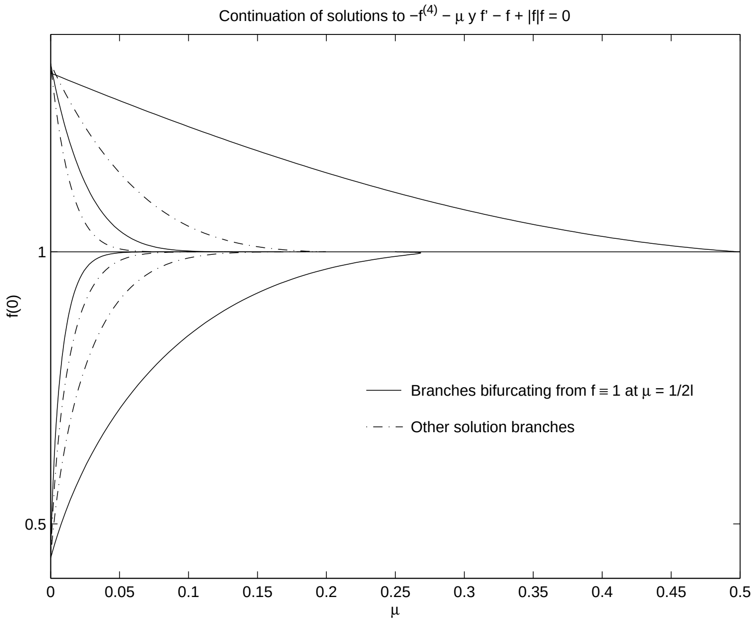

FIG. 6.1. *Bifurcation diagram for $m = 2$.*

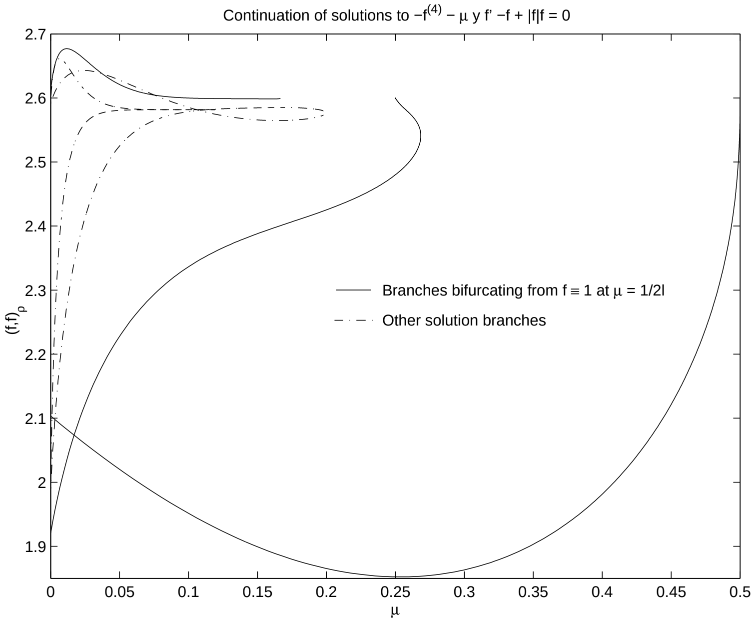

FIG. 6.2. *Bifurcation diagram for $m = 2$ in L^2_ρ.*

subscript s denotes stable, see Section 7) of (4.12) for the value of $\mu_2 = 1/4$. This solution gives a self-similar solution of the underlying PDE (1.7). In Figure 6.3 we compare the numerical solution to the boundary-value problem (2.9), (2.10) with the asymptotic construction (5.27). In Figure 6.4 we present an enlargement of Figure

6.1 close to the point $\mu = 1/2$ allowing a direct comparison with the asymptotic calculation of $f(0)$ given by (5.28).

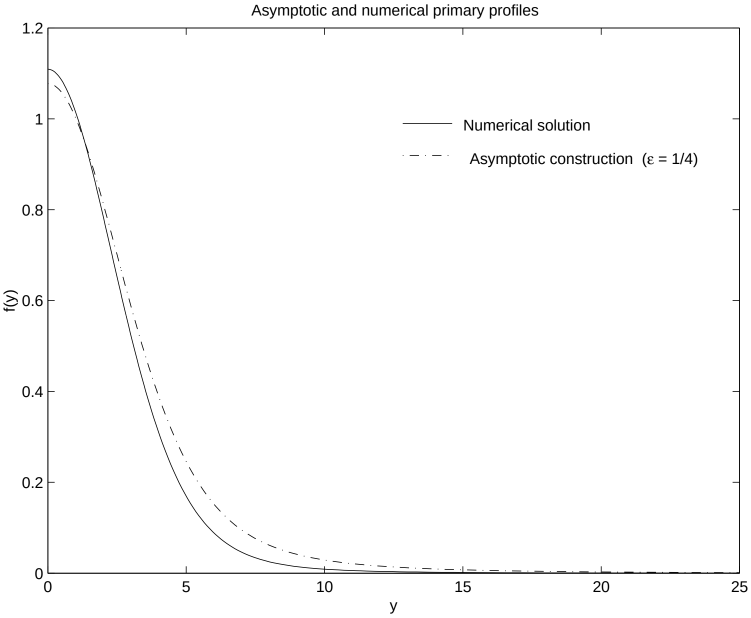

FIG. 6.3. *Comparison of asymptotic and numeric solutions.*

In contrast, the curve bifurcating from $\mu = 1/4$ appears to exist for all $\mu \in [0, 1/4 + \delta]$, where δ is a small positive constant. This behaviour can be seen more clearly in the enlargement of Figure 6.1 close to $\mu = 1/4$ which is presented in Figure 6.4. Again, we can compare this figure to the asymptotic calculation of $f(0)$ given by (5.36), and the associated discussion on the unstable centre manifold behaviour in Section 5, which predicts the existence of the bifurcating curve for a range of values of $\varepsilon > 1/4$. This asymptotic calculation is clearly only valid for a small range of values of $\mu > 1/4$, and the curve of solutions folds back at $\mu \simeq 0.26841\ldots$.

In particular, we observe a second non-zero solution $f_u(y)$ (the subscript u denotes unstable, see Section 7) of (4.12) at $\mu = 1/4$. The existence of this solution implies the existence of a further self-similar solution of the PDE. As remarked earlier, this result is consistent with the semi-stability of the centre manifold when $m = 2$. The profiles of the two distinct self-similar solutions $f_s(y)$ and $f_u(y)$ are given in Figure 6.5.

Observe that the form of $f_s(y)$ is qualitatively similar to the profile of the solution computed close to $\mu = 1/2$ and described asymptotically in the previous section. In particular, it appears to be a monotone decreasing function of y. In contrast, the self-similar solution $f_u(y)$ is *increasing* for small values of y and decreasing for larger values. This possible small non-monotonicity in the expansion (5.35) is described by the terms $O(\varepsilon^2)$.

We also present in Figure 6.4 a detail of the neighbourhood of $\mu = 1/6$. Although this branch does not lead to a self-similar solution, its local form is interesting. As predicted by the asymptotic analysis, it bifurcates to the left, but then folds back twice locally before continuing backwards to $\mu = 0$.

Following these calculations we make the conjecture

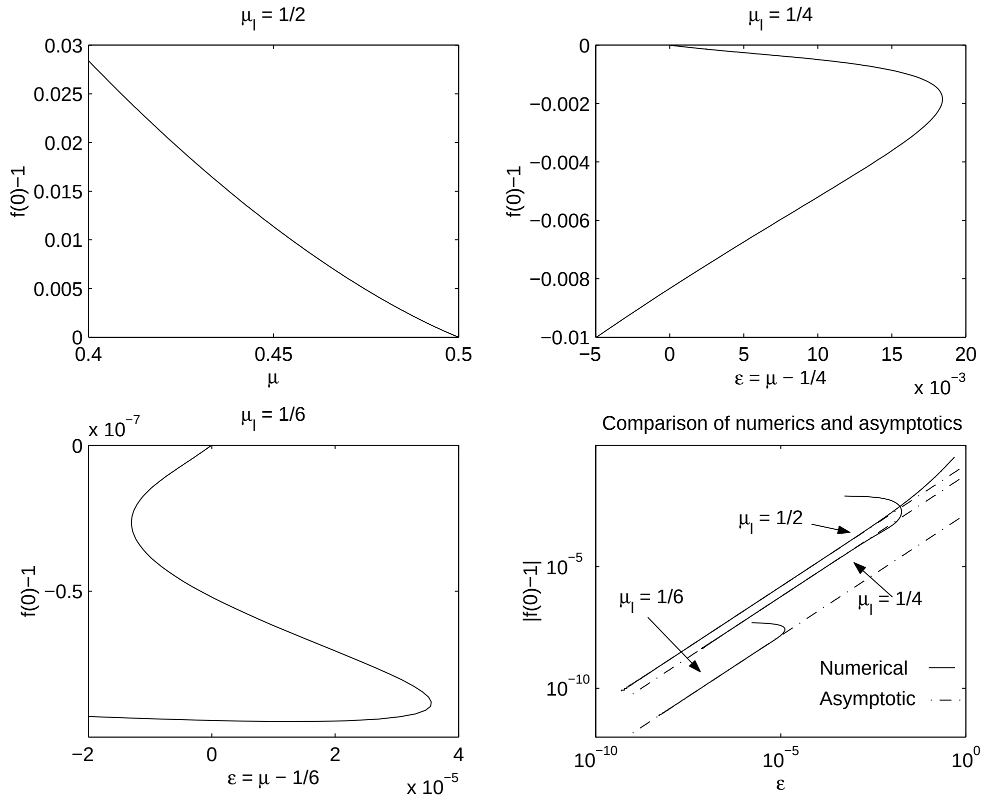

FIG. 6.4. *Detail of branches at $\mu = 1/2, 1/4, 1/6$ for $m = 2$ and $p = 2$.*

CONJECTURE 6.1. *If $m = 2$, then each of the curves bifurcating from the point $\mu_l = 1/2l$ continues globally to include the point $\mu = 0$, and has $l - 1$ fold bifurcations in the vicinity of $\mu = 1/2l$.*

Such fold bifurcations can occur, [33], if

$$0 \in \sigma(\boldsymbol{\mathcal{L}}_\mu + G'(f)I). \tag{6.1}$$

This equation determines a difficult eigenvalue problem for higher-order operators with non-constant coefficients. The eigenvalues of this problem correspond to the turning points of the solution branches indicated in Figure 6.4.

Lastly, in Figure 6.4 we compare our asymptotic construction of the bifurcation diagram with the numerical computations. Away from all folds, the agreement is excellent even with only a linear approximation.

6.2. The sixth-order case $m = 3$. A bifurcation diagram is similar to Figure 6.1, and now for the case of the sixth order differential equations when $m = 3$ is presented in Figure 6.6. The far field boundary condition is (5.4).

This picture is qualitatively similar to Figure 6.1, with the solutions at $\mu_3 = 1/6$ of interest. As before, the monotone decreasing (in a neighbourhood of the origin) solution bifurcating from $\mu = 1/2$ extends backwards to $\mu_3 = 1/6$ as does the solution bifurcating from $\mu = 1/4$. This leads to two self-similar solutions f_s and f_u. A detail

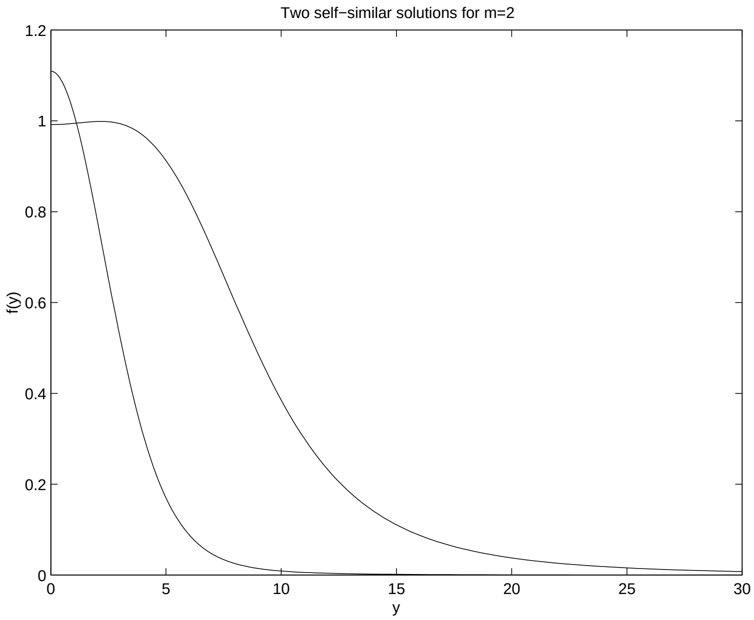

FIG. 6.5. *The two self-similar profiles f_s, f_u for $m = 2$.*

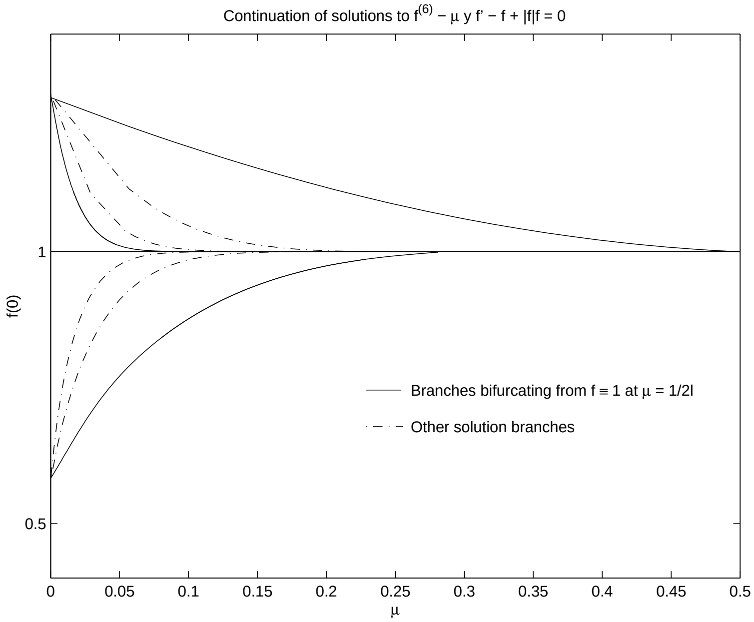

FIG. 6.6. *Bifurcation diagram for $m = 3$.*

of Figure 6.6 in the neighbourhood of $\mu = 1/6$ is given in Figure 6.7. As predicted by the asymptotic analysis of Section 5, this curve bifurcates *to the left* and there are no non-zero (and hence no self-similar) solutions on this branch when $\mu = 1/4$. Consistent with the previous analysis, we observe two self-similar solutions associated with the unstable sub-space and none associated with the centre subspace.

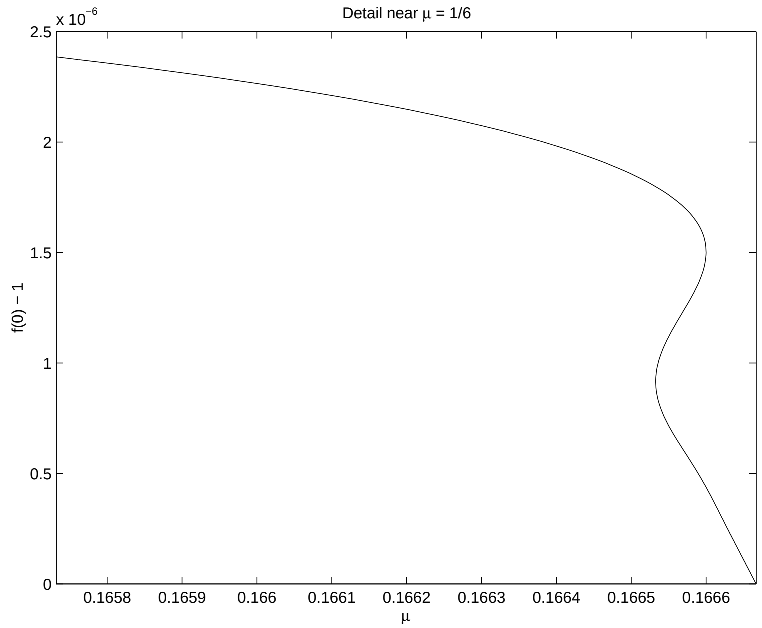

FIG. 6.7. *Detail of bifurcation diagram for* $m = 3$ *near* $\mu = 1/6$.

A plot of f_s and f_u is given in Figure 6.8. It is of special interest that for this value of m we see *four* other self-similar solutions that arise from paths which start at $\mu = 0$. These are also plotted in Figure 6.7. Observe that $2 + 4 = 6 = m(m-1)$ for $m = 3$, cf. the last comment in Section 4.

7. Numerical simulations of the solutions of the PDE.

Whilst the self-similar solutions of (1.7) and (1.6) are important, they only give a partial picture of the overall dynamical behaviour of the solutions of these systems. For example, we have not even established whether the self-similar solutions are stable. As we have mentioned, for $m > 1$, the operators in (2.5) and (2.7) are not potentials and do not generate gradient flows as in the second-order case. For $m = 1$, a Lyapunov function exists and this essentially simplifies the asymptotic analysis, see the first results in [22] for $N = 1$ and [26, 27] for $N \geq 1$. Moreover, compactness of the rescaled orbits $\{\theta(\tau), \tau > \tau_0\}$ remains an open problem (the only known L^∞-estimate for the blow-up rate is a lower one, [10], [21]). This makes the asymptotic stability for higher-order equations extremely difficult.

In this section we investigate the dynamics of (1.7) in the case of $m = 2$ by using a *scale-invariant* adaptive numerical method. A general description of the philosophy and implementation of these methods is given in [31, 9, 45] and the references therein. Scale-invariant methods are extremely well suited to computing the solution of systems of PDEs which have solutions blowing up in finite time and which are also invariant under the action of scaling symmetries. In particular, the underlying PDE is semi-discretized in *space* by using a collocation method on a moving grid. This leads to a system of (stiff) ODEs which are then solved by using a BDF method. The spatial

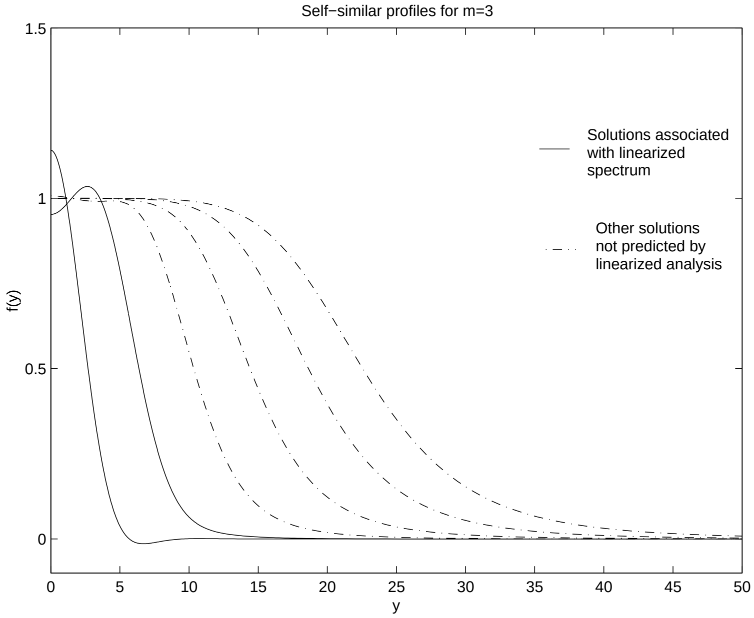

FIG. 6.8. *Six self-similar profiles for $m = 3$, of which two arise from the analytic bifurcation analysis and four which do not.*

grid is chosen to *equidistribute* a monitor function $M(u)$ chosen to be

$$M(u) = |u|^{p-1}. \tag{7.1}$$

By doing this, mesh points are clustered where $M(u)$ and hence u is large. The particular choice of $M(u)$ given above leads to a discrete system of equations which is invariant to changes in the scale of the solution and gives relative truncation errors which are *independent of scale.* This is the key to the accuracy of the numerical calculations of this section.

Example 1. For the first calculation we consider the polynomial nonlinearity in (1.7) with as initial data the function

$$u_0(x) = 2e^{-x^2}.$$

Firstly, we present the evolution of this data in the original variables in Figure 7.1, here the formation of the singularity can be seen clearly. In Figure 7.2 we present *the same* data, this time in the scaled variables θ and y. Here, the blow-up time T is estimated by a least squares fit of $u(0,t) = f_0/(T-t)^{1/(p-1)}$ with both f_0 and T unknown. The most significant aspect of this figure is that the solutions rapidly converge (exponentially in τ) to the first monotone function $f_s(y)$. The solution of the ODE (2.9) is plotted on Figure 7.2 for comparison and is indistinguishable from the large τ solutions to the full PDE.

Example 2. For our final calculation, we take as initial data the second solution to (2.9), the solution which extends from the bifurcation point $\mu_2 = 1/4$,

$$u(x,0) = f_u(x).$$

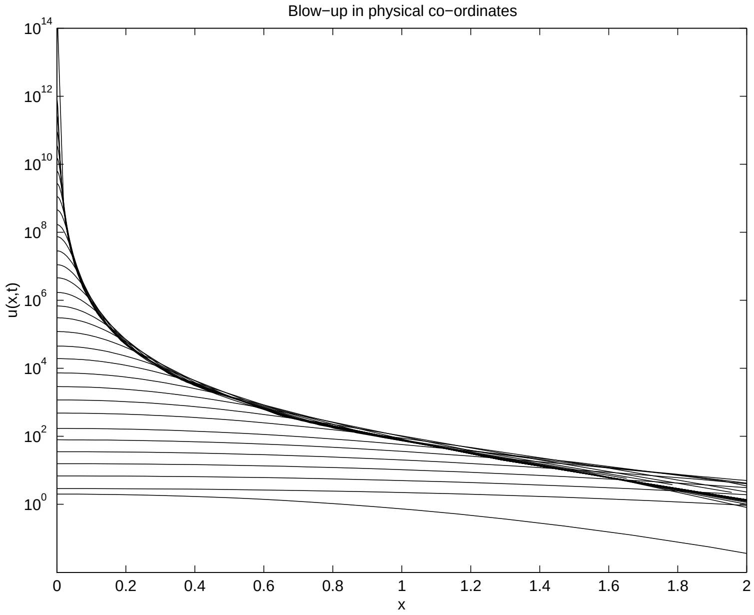

FIG. 7.1. *The solution of (1.7) in the physical variables.*

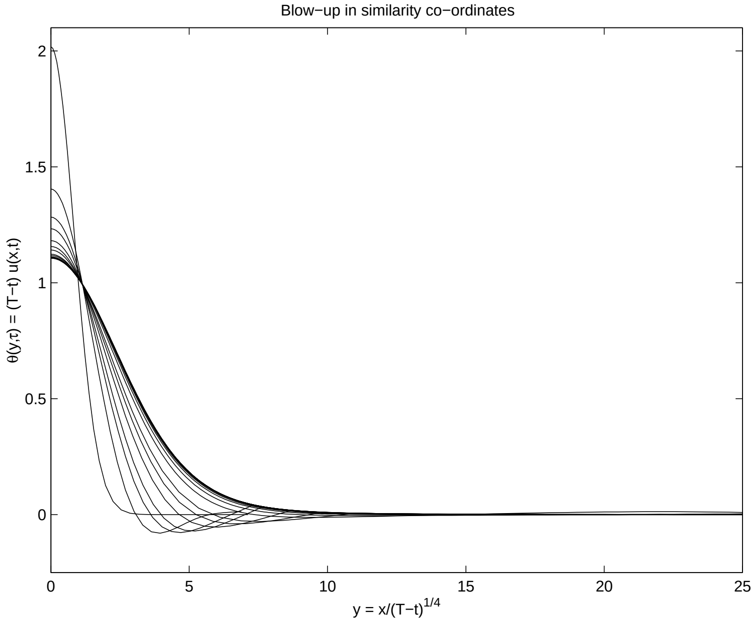

FIG. 7.2. *The solution of (1.7) in the rescaled variables.*

This is seen to be unstable. While remaining close to the initial data as the PDE solution increases over several orders of magnitude, eventually the rescaled solution converges to the primary profile as in Example 1, see Figure 7.3.

Calculations have also been done for the case of the exponential nonlinearity and

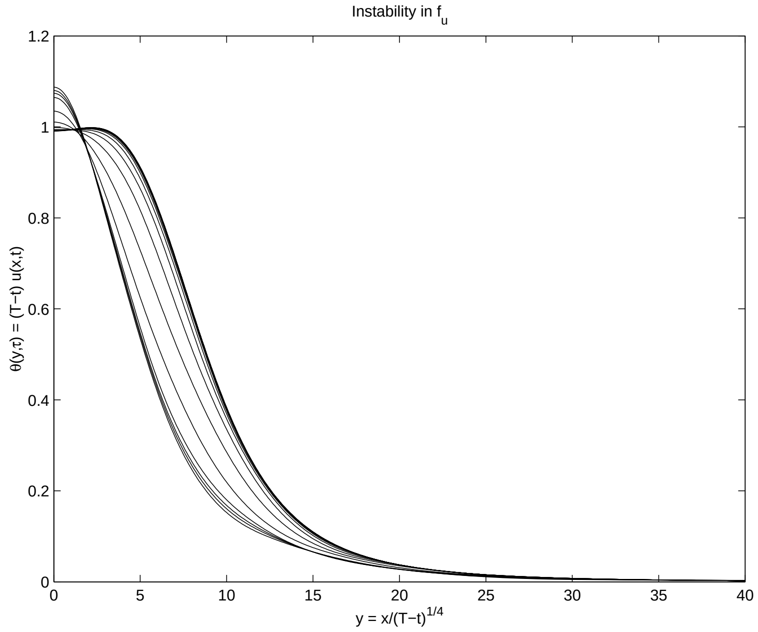

FIG. 7.3. *The solution of (1.7) in the rescaled variables.*

are fundamentally the same as those presented here, see also [24].

8. Conclusions.

It is clear from this study that the (self-similar) behaviour of the blow-up solutions of a relatively straightforward higher-order partial differential equation is quite different, and in a sense simpler, than that of related second-order equations. It is very likely that similar behaviour will be observed in a much wider class of higher-order equations. The numerical and asymptotic calculations presented in this paper have suggested a number of open questions in analysis which deserve further investigation, in particular, a fully rigorous proof of the existence of the self-similar solutions and the uniqueness and stability of the "most" monotone stable profiles. We leave this as a subject for future study.

Acknowledgments. The authors wish to thank J.F. Toland for several useful discussions.

REFERENCES

[1] M. M. Ad'jutov and L. A. Lepin, *Absence of blowing up similarity structures in a medium with a source for constant thermal conductivity*, Differ. Equat., 20 (1984), pp. 1279–1281.
[2] C. J. Amick and J. F. Toland, *Homoclinic orbits in the dynamic phase space analogy of an elastic strut*, Euro. J. Appl. Math., 3 (1992), pp. 97–114.
[3] S. B. Angenent, *The Morse-Smale property for a semi-linear parabolic equation*, J. Differ. Equat., 62 (1986), pp. 427–442.
[4] G. I. Barenblatt, *Scaling, Self-similarity, and Intermediate Asymptotics*, Cambridge University Press, Cambridge, 1996.
[5] J. Bebernes and D. Eberly, *Mathematical Problems from Combustion Theory*, Springer-Verlag, New York, 1989.
[6] M. Ben-Artzi, H. Koch, and J. C. Saut, *Dispersion estimates for fourth order Schrödinger equations*, C. R. Acad. Sci. Paris Série I Math., 330 (2000), pp. 87–92.
[7] A. Bressan, *Stable blow-up patterns*, J. Differ. Equat., 98 (1992), pp. 57–75.

[8] C. J. Budd and V. A. Galaktionov, *Stability and spectra of blow-up in problems with quasilinear gradient diffusivity*, Proc. Roy. Soc. London A, 454 (1998), pp. 2371–2407.

[9] C. J. Budd, W. Huang, and R. D. Russell, *Moving mesh methods for problems with blow-up*, SIAM J. Sci. Comput., 17 (1996), pp. 305–327.

[10] M. Chaves and V. A. Galaktionov, *Regional blow-up for a higher-order semilinear parabolic equation*, Euro. J. Appl. Math., 12 (2001), pp. 601–623.

[11] M. Chen, X. Y. Chen, and J. K. Hale, *Structural stability for time-periodic one-dimensional parabolic equations*, J. Differ. Equat., 96 (1992), pp. 355–418.

[12] E. A. Coddington and N. Levinson, *Theory of Ordinary Differential Equations*, McGraw-Hill Book Company, Inc., New York/London, 1955.

[13] E. J. Doedel, *Auto, a program for the automatic bifurcation analysis of autonomous systems*, Cong. Numer., 30 (1981), pp. 265–384.

[14] Y. V. Egorov, V. A. Galaktionov, V. A. Kondratiev, and S. Pohozaev, *On the necessary conditions of existence to a quasilinear inequality in the half-space*, Comptes Rendus Acad. Sci. Paris, 330 (2000), pp. 93–98.

[15] Y. V. Egorov, V. A. Galaktionov, V. A. Kondratiev, and S. I. Pohozaev, *Asymptotic behaviour of global solutions to higher-order semilinear parabolic equations in the supercritical range*. submitted to Comm. Partial Differ. Equat.. (Report on web server: `http//mip.ups-tlse.fr`), 2002.

[16] S. D. Eidelman, *Parabolic Systems*, North-Holland Publ. Comp., Amsterdam/London, 1969.

[17] G. Fibich, B. Ilan, and G. Papanicolau, *Self-focusing with fourth-order dispersion*, SIAM J. Appl. Math, 62 (2002), pp. 1437–1462.

[18] S. Filippas and R. V. Kohn, *Refined asymptotics for the blow-up of* $u_t - \Delta u = u^p$, Comm. Pure Appl. Math., 45 (1992), pp. 821–869.

[19] D. A. Frank-Kamenetskii, *Towards temperature distributions in a reaction vessel and the stationary theory of thermal explosion*, Doklady Acad. Nauk SSSR, 18 (1938), pp. 411–412.

[20] V. A. Galaktionov, *On a spectrum of blow-up patterns for a higher-order semilinear parabolic equations*, Proc. Roy. Soc. London A, 457 (2001), pp. 1623–1643.

[21] V. A. Galaktionov and S. I. Pohozaev, *Existence and blow-up for higher-order semilinear parabolic equations: majorizing order-preserving operators.* Indiana Univ. Math. J., to appear.

[22] V. A. Galaktionov and S. A. Poshashkov, *Application of new comparison theorems to the investigation of unbounded solutions of nonlinear parabolic equations.*, Diff. Equat., 22 (1986), pp. 809–815.

[23] V. A. Galaktionov and J. L. Vazquez, *The problem of blow-up in nonlinear parabolic equations*, Discr. Cont. Dyn. Syst., 8 (2002), pp. 399–433.

[24] V. A. Galaktionov and J. F. Williams, *Blow-up in a fourth-order semilinear parabolc equation from convection explosion theory.* Submitted to Euro J. Appl. Math, 2002.

[25] I. M. Gel'fand, *Some problems in the theory of quasilinear equations*, Amer. Math. Soc. Transl. (Ser. 2), 29 (1963), pp. 295–381. See Section 15 by G.I. Barenblatt.

[26] Y. Giga and R. Kohn, *Asymptotically self-similar blow-up of semilinear heat equations*, Comm. Pure Appl. Math., 38 (1985), pp. 297–319.

[27] Y. Giga and R. Kohn, *Characterizing blowup using similarity variables*, Indiana Univ. Math. J., 36 (1987), pp. 1–40.

[28] D. Henry, *Some infinite-dimensional Morse-Smale systems defined by parabolic partial differential equations*, J. Differ. Equat., 59 (1985), pp. 165–205.

[29] M. A. Herrero and J. J. L. Velázquez, *Blow-up behaviour of one-dimensional semilinear parabolic equations*, Inst. Henri Poincaré, Analyse non linéaire, 10 (1993), pp. 131–189.

[30] L. Hocking, K. Stewartson, and J. Stuart, *A nonlinear instability burst in plane parallel flow*, J. Fluid Mech., 51 (1972), pp. 702–735.

[31] W. Huang and R. Russell, *A moving collocation method for solving time dependent partial differential equations*, Appl. Num. Math., 20 (1996), pp. 101–116.

[32] G. Joulin, A. Mikishev, and G. I. Sivashinsky, *A Semenov-Rayleigh-Benard problem.* Preprint.

[33] M. A. Krasnosel'skii, *Topological Methods in the Theory of Nonlinear Integral Equations*, Pergamon Press, Oxford/Paris, 1964.

[34] H. A. Levine, *The role of critical exponents in blow-up problems*, SIAM Review, 32 (1990), pp. 262–288.

[35] A. Lunardi, *Analytic Semigroups and Optimal Regularity in Parabolic Problems*, Birkhäuser, Basel/Berlin, 1995.

[36] F. Merle and H. Zaag, *Stability of the blow-up profile for equations of the type* $u_t = \Delta u +$

$|u|^{p-1}u$, Duke Math. J., 86 (1997), pp. 143–195.

[37] E. Mitidieri and S. I. Pohozaev, *A priori estimates and blow-up of solutions to nonlinear partial differential equations and inequalities*, Proc. Steklov Math. Inst., 234 (2001). ISSN: 0081-5438.

[38] L. Peletier and W. Troy, *Spatial Patterns: Higher-order Models in Physics and Mechanics*, Birkhäuser, 2001.

[39] A. A. Samarskii, V. A. Galaktionov, S. P. Kurdyumov, and A. P. Mikhailov, *Blow-up in Quasilinear Parabolic Equations*, Walter de Gruyter, Berlin/New York, 1995.

[40] L. F. Shampine and J. Kierzenka, *A BVP solver based on residual control and the MATLAB PSE*, ACM T Math. Software, 27 (2001), pp. 299–316.

[41] C. Sulem and P. L. Sulem, *The Nonlinear Schrödinger Equation*, vol. 139 of Appl. Math. Sci., Springer-Verlag, Berlin, 1999.

[42] M. A. Vainberg and V. A. Trenogin, *Theory of Branching of Solutions of Non-Linear Equations*, Noordhoff Int. Publ., Leiden, 1974.

[43] J. J. L. Velazquez, *Estimates on $(N-1)$-dimensional Hausdorff measure of the blow-up set for a semilinear heat equation*, Indiana Univ. Math. J., 42 (1993), pp. 445–476.

[44] J. J. L. Velázquez, V. A. Galaktionov, and M. A. Herrero, *The space structure near a blow-up point for semilinear heat equations: a formal approach*, USSR Comput. Math. Math. Phys., 31 (1991), pp. 46–55.

[45] J. F. Williams, X. Xu, and R. D. Russell, *MovCol4: A moving collocation method for higher-order parabolic equations, in preparation.*

[46] Y. B. Zel'dovich, G. I. Barenblatt, V. B. Librovich, and G. M. Makhviladze, *The Mathematical Theory of Combustion and Explosions*, Consultants Bureau (Plenum), New York/London, 1985.

[47] Y. B. Zel'dovich and Y. P. Raizer, *Physics of Shock Waves and High-Temperature Hydrodynamic Phenomena* Vols I and II, Academic Press, New York, 1966.